



## OPEN ACCESS

## EDITED BY

Craig C. McLauchlan,  
Illinois State University, United States

## REVIEWED BY

Sajjad Hussain Sumra,  
University of Gujrat, Pakistan  
Abdulmajeed A. M. Alezzy,  
University of Mysore, India  
Christopher Daley,  
University of San Diego, United States

## \*CORRESPONDENCE

Norah Barba-Behrens,  
✉ norah@unam.mx

RECEIVED 31 October 2025

REVISED 11 December 2025

ACCEPTED 23 December 2025

PUBLISHED 05 February 2026

## CITATION

Fugarolas W, Reyes-Carmona L,  
Landeros-Rivera B, Almaguer-Flores A and  
Barba-Behrens N (2026) Design, synthesis,  
reactivity, and biological activity of  
nitroimidazole derivatives and their copper(II)  
coordination compounds.  
*Front. Chem. Biol.* 4:1736242.  
doi: 10.3389/fchbi.2025.1736242

## COPYRIGHT

© 2026 Fugarolas, Reyes-Carmona, Landeros-  
Rivera, Almaguer-Flores and Barba-Behrens.  
This is an open-access article distributed under  
the terms of the [Creative Commons Attribution  
License \(CC BY\)](https://creativecommons.org/licenses/by/4.0/). The use, distribution or  
reproduction in other forums is permitted,  
provided the original author(s) and the copyright  
owner(s) are credited and that the original  
publication in this journal is cited, in accordance  
with accepted academic practice. No use,  
distribution or reproduction is permitted which  
does not comply with these terms.

# Design, synthesis, reactivity, and biological activity of nitroimidazole derivatives and their copper(II) coordination compounds

Walter Fugarolas<sup>1</sup>, Lorena Reyes-Carmona<sup>2</sup>,  
Bruno Landeros-Rivera<sup>1</sup>, Argelia Almaguer-Flores<sup>2</sup> and  
Norah Barba-Behrens<sup>1\*</sup>

<sup>1</sup>Departamento de Química Inorgánica, Facultad de Química, Universidad Nacional Autónoma de México, Ciudad Universitaria, Ciudad de México, Mexico, <sup>2</sup>Laboratorio de Biointerfases, División de Estudios de Posgrado e Investigación, Facultad de Odontología, Universidad Nacional Autónoma de México, Ciudad de México, Mexico

In the last 60 years, the broad spectrum of activity of nitroimidazole derivatives against anaerobic bacteria, parasites, and protozoa has permitted their use as the first choice of treatment for many infectious diseases. New compounds are needed to overcome the acquired resistance of bacteria and parasites. This work aimed to investigate 4- and 5-nitroimidazole derivatives in terms of the contribution of the position of the nitro group, along with that of different substituents, on their chemical, structural, and biological properties. Copper (II) coordination compounds with these derivatives were synthesized and characterized by analytical and spectroscopical techniques. Their structural properties and their intra- and intermolecular interactions were analyzed from single crystal X-ray diffraction studies. Theoretical calculations allowed for explaining the lability in solution of the copper (II) coordination compounds with the 4-nitroimidazole derivatives. The potential antimicrobial activity against anaerobic periodontal and opportunistic aerobic bacteria, including *E. coli*, *S. aureus*, *S. mutans*, and *P. gingivalis*, was evaluated. It is noteworthy that the position of the nitro group in the heterocycle drives their coordination behavior toward the metal ions, the geometry of the copper (II) atom in the complexes, and their stability in solution, thus affecting their biological activity.

## KEYWORDS

4-nitroimidazole, 5-nitroimidazole, coordination behavior, copper(II) complexes, non-covalent interactions, periodontal bacteria, reactivity

## 1 Introduction

Imidazole is a biologically relevant heterocycle found in the amino acid histidine. It is present in various pharmaceutical agents with a wide range of applications, including antifungals, antibiotics, antiparasitics, radiotracers, analgesics, and anti-inflammatory therapies (Poyraz et al., 2024). Particularly, nitroimidazole derivatives have become first-line drugs for the treatment of various infectious diseases, with their biological activity largely driven by the position of the nitro group. The azomycin, 2-nitroimidazole, shown in Figure 1, was the first derivative to be isolated from *Streptomyces* bacteria, which

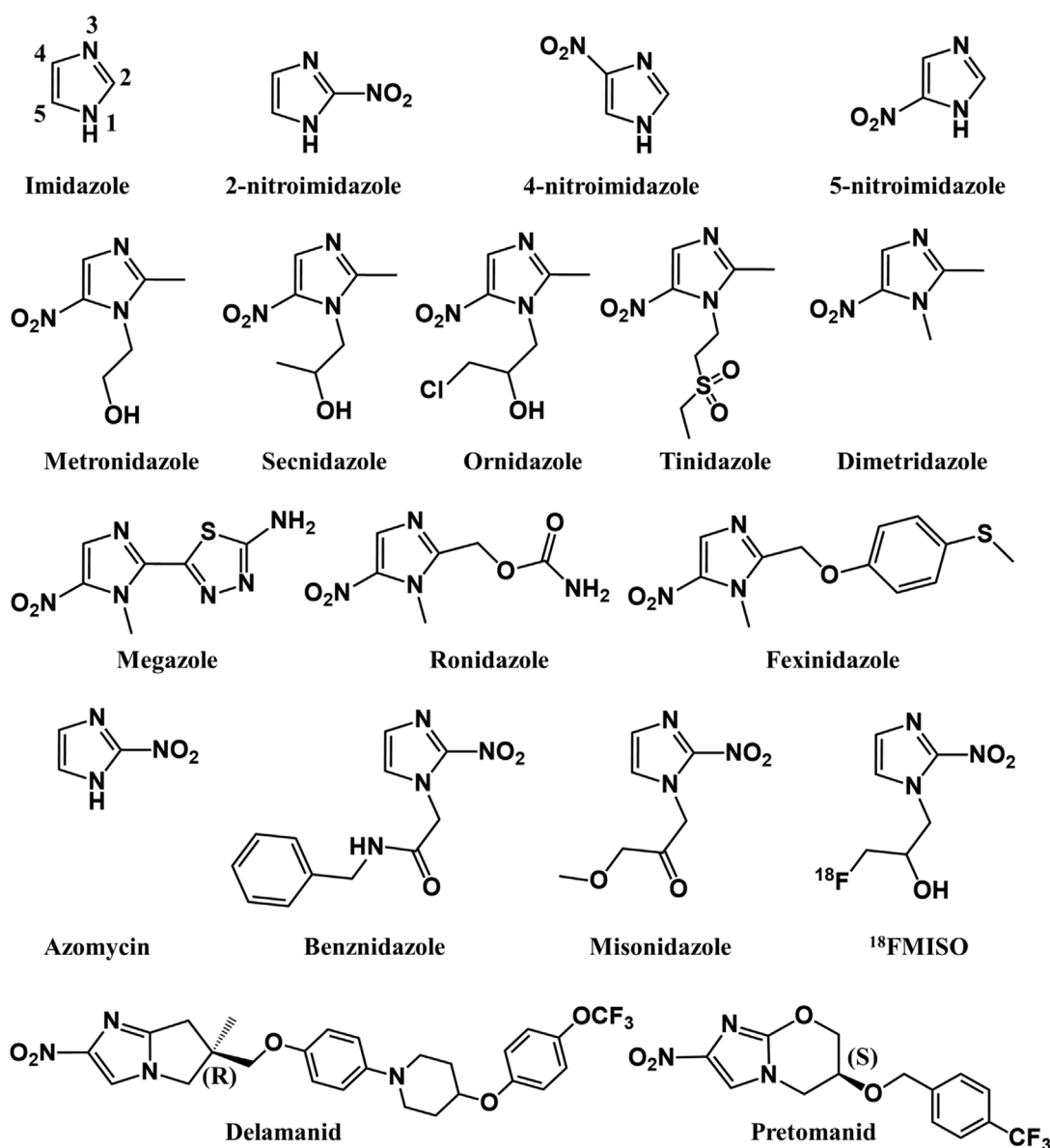
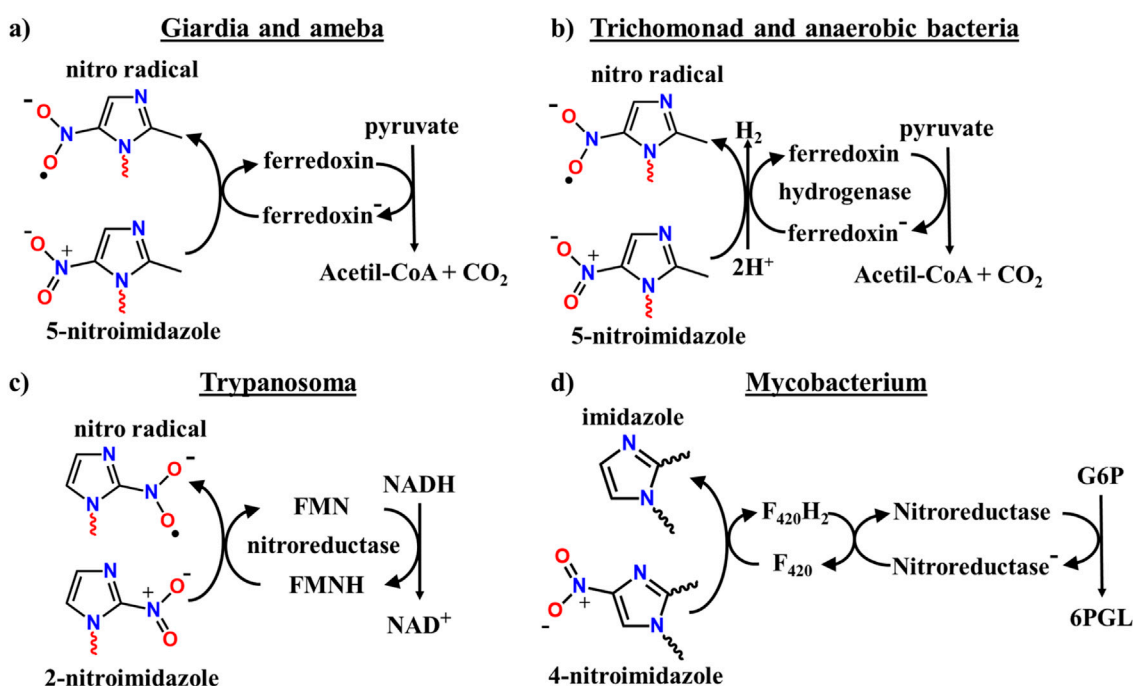


FIGURE 1  
Chemical structures of 2-, 4-, and 5-nitroimidazole derivatives used to treat various infectious diseases.

exhibited a broad spectrum of activity against several bacteria and *Trichomonas vaginalis* (Nakamura, 1955; Lancini and Lazzari, 1965). However, its complex synthesis and low yields led to the development of 5-nitroimidazole derivatives. More than one hundred 5-nitroimidazole derivatives were synthesized as potential alternatives to the natural product azomycin (Anonymous, 1978). Among them, metronidazole (mnz), shown in Figure 1, demonstrated the best balance between efficacy and toxicity. Starting in the 1960s, mnz has become a systemic treatment for parasitic infections caused by *T. vaginalis*, *Giardia lamblia*, and *Entamoeba histolytica*. In the 1980s, its use was expanded to include the treatment of non-spore-forming anaerobic bacterial infections caused by *Bacteroides* and *Clostridium* species (Rolfe and Finegold, 1981), and 10 years later, it was well established as an effective therapy for oral infections such as

gingivitis and periodontitis (Loesche et al., 1992; Greenstein, 1993). Currently, it remains as a first-line therapeutic agent, with a broad spectrum against bacteria and parasites (Freeman et al., 1997; Löfmark et al., 2010; Suárez et al., 2024). Due to the success of mnz, a second generation of 2-methyl-5-nitroimidazoles, tinidazole, ornidazole, secnidazole, and dimetridazole (Figure 1), was developed in the late 1960s. They showed good biological activity, although the change of the substituent in the N1 position gave rise to different pharmacokinetics (Goldman, 1982) and metabolites (Wood et al., 1986; Granja et al., 2013). They have been mainly used in the treatment and prevention of parasitic infections, while 1-methyl-5-nitroimidazole derivatives (megazole, ronidazole, and fexinidazole; Figure 1) extended the 5-nitroimidazole spectrum of action to *Trypanosoma* parasites (Ang et al., 2017).



**FIGURE 2**  
Metabolic pathways of nitroimidazoles in different microorganisms: (a,b) 1e-reduction of the nitro group in 5-nitroimidazole derivatives; (c) 1e-reduction of the nitro group in 2-nitroimidazole derivatives; (d) loss of the nitro group in 4-nitroimidazole derivatives (Samuelson, 1999; Wilkinson et al., 2008; Mudde et al., 2022).

In the search for new biological activity, 2-nitroimidazole derivatives were synthesized: misonidazole, benznidazole, and  $^{18}\text{F}$ -fluoromisonidazole (Müller-Kratz et al., 2018; Ruan et al., 2023). Benznidazole has shown to be effective against *Trypanosoma cruzi* and is a first-choice drug for Chagas disease. The toxicity of misonidazole and  $^{18}\text{F}$ -fluoromisonidazole, even though they were active as radiosensitizers, prevented their use in pharmacology (Rajendran and Krohn, 2005).

Finally, in the past decade, two 4-nitroimidazole derivatives were FDA approved in the treatment of resistant tuberculosis strains, pretomanid and delamanid. Both molecules are fused heterocycles, imidazooxazine and imidazooxazole, respectively, designed with substituents that inhibit the synthesis of mycolic acids, whereas the nitro group is crucial for the biological activity by generating reactive nitrogen species (Mudde et al., 2022), as shown in Figure 1.

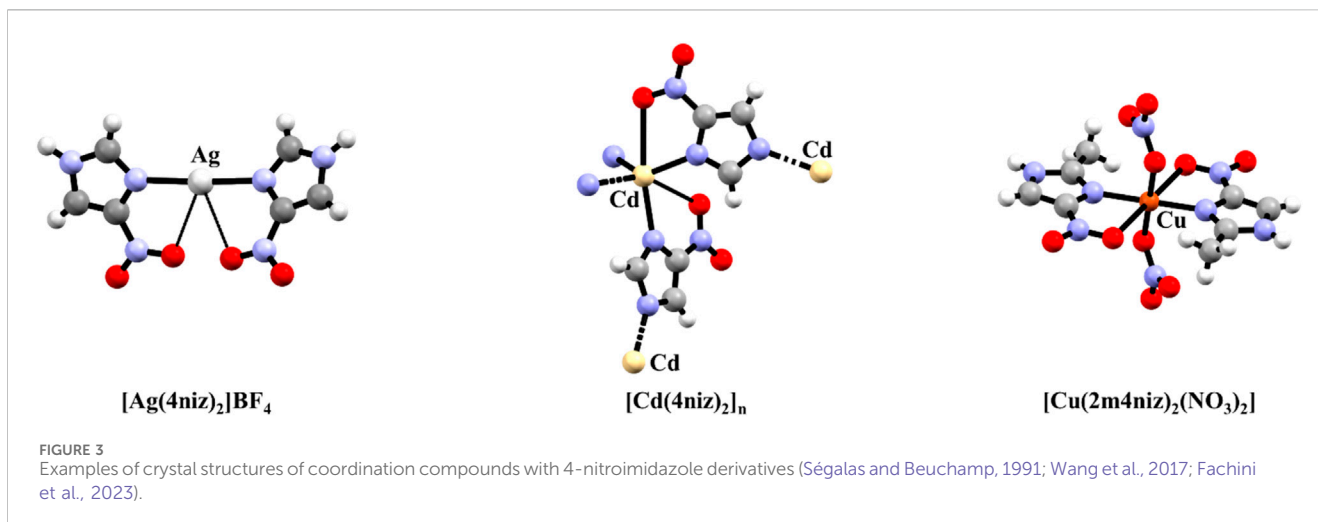
The broad spectrum of nitroimidazole therapeutics is due to their mechanism of action. All nitroimidazole derivatives present a similar mechanism as they are prodrugs that require bioactivation inside the microorganisms. For the 2- and 5-nitroimidazoles, there are three steps in the mechanism: 1. Access to the cell via passive diffusion. 2. Activation through a one-electron (type II) or two-electron (type I) reduction of the nitro group, stabilizing the nitrogen active species. 3. Cell damage (Ang et al., 2017; Nepali et al., 2019; Lauwaet et al., 2020; Vichi-Ramírez et al., 2024). On the other hand, for the 4-nitroimidazole, it has been proposed that the nitro group is lost in the bioactivation (Mudde et al., 2022). Although they have similar mechanisms of action, the position of the nitro group in the heterocycle gives place to diverse metabolism pathways of the drugs (Figure 2), and different

redox potentials for the one-electron reversible reduction of the nitro group, 2-nitroimidazole (ca.  $-390$  mV(SCE)), 5-nitroimidazoles (ca.  $-475$  mV(SCE)), and 4-nitroimidazole (ca.  $-520$  mV(SCE)) (Wardman and Clarke, 1975).

An alternative to the development of novel organic drugs is coordination compounds. There are three main strategies in the design of novel metallodrug agents (Gambino and Otero, 2019):

1. Select bioactive molecules as ligands with different transition metals, aiming for a synergic effect or even to expand the spectrum of the drug.
2. Specific targeting to biomolecules such as DNA or proteins. Favor the cleavage of the coordination compound *via* non-covalent interaction through the ligands or covalent bonding through the metal center.
3. Design coordination compounds that act as chaperones for the metal or ligand.

A variety of coordination compounds with 2-methyl-5-nitroimidazole derivatives have been reported to enhance and expand the spectrum of biological activity of the nitroimidazole drug family (Navarro-Peñaloza et al., 2023a). Among these, the metronidazole metal complexes have been developed. The compound  $[\text{Cu}_2(\text{mnz})_4(\text{H}_2\text{O})_2(\mu\text{-Cl})_2]\text{Cl}_2$  was active against *E. histolytica* (Bharti et al., 2002), while silver(I) complexes have shown antifungal and promising antibacterial activity (Kalinowska-Lis et al., 2015; Radko et al., 2019). In recent years, zinc(II), copper(II), and silver(I) salicylate-mnz complexes have been shown to be effective agents against both Gram-positive and Gram-negative bacteria, including biofilm-forming strains (Contini



et al., 2025). In all cases, the metal complexes were more active than the ligands or the metal salts by themselves. Other 5-nitroimidazole coordination compounds presented novel antiparasitic activity, such as the tinidazole (5tnz) copper (II) compound [Cu(5tnz)<sub>2</sub>Br<sub>2</sub>], which showed an anthelmintic activity against *Dactylogyrid monogeanis* parasites (Castro-Ramírez and Barba-Behrens, 2025), while zinc(II) and copper (II) compounds with ornidazole, [M(onz)<sub>2</sub>Cl<sub>2</sub>] and [M(onz)<sub>2</sub>Br<sub>2</sub>], presented a promising activity against *Toxoplasma gondii* (Navarro-Peñaloza et al., 2023b). Neither the ligand nor the metal salts were active under similar conditions.

In contrast to the 5-nitroimidazole derivatives, few examples of 2- and 4-nitroimidazole coordination compounds have been reported. The coordination behavior of 2-nitroimidazole was first investigated with platinum (II) (Bales et al., 1985; Rochon et al., 1991) and palladium (II) (Rochon and Melanson, 1993), and as a linker in cobalt (II) metal-organic frameworks (Biswal et al., 2012). Nevertheless, the main application of 2-nitroimidazoles has been in radiopharmaceuticals for hypoxic cells (such as tumoral cells), as a side chain functional group on coordination compounds with <sup>10</sup>B, Al, <sup>64</sup>Cu, <sup>99</sup>Tc, and <sup>68</sup>Gd (Nguyen and Kim, 2023; Mittal and Mallia, 2023; Mittal et al., 2024; Ozasa et al., 2025).

For 4-nitroimidazole, the platinum (II) compounds with 1,2-dimethyl-4-nitroimidazole (4dmz) and 1-(2'-hydroxyethyl)-2-methyl-4-nitroimidazole (4mnz) (Bales et al., 1985) were the first reported complexes. There are some X-ray crystal structures of coordination compounds with 4-nitroimidazole (4niz): [Ag(4niz)<sub>2</sub>]NO<sub>3</sub>, [Ag(4niz)<sub>2</sub>]BF<sub>4</sub> (Ségalas and Beuchamp, 1991), [Cu(4niz)<sub>2</sub>(H<sub>2</sub>O)<sub>2</sub>](NO<sub>3</sub>)<sub>2</sub> (Atria et al., 2011), and recently, the polymeric imidazolate cadmium (II) compound [Cd(4niz)<sub>2</sub>]<sub>n</sub> (Wang et al., 2017); with 2-methyl-4-nitroimidazole (2m4niz): [Cu(2m4niz)Cl<sub>2</sub>] (Barba-Behrens et al., 1991), [Cu(2m4niz-COO)<sub>2</sub>] (Goodgame et al., 1992), [Cu(2m4niz)<sub>2</sub>(NO<sub>3</sub>)<sub>2</sub>] and [Cu(2m4niz)<sub>2</sub>(H<sub>2</sub>O)<sub>2</sub>](NO<sub>3</sub>)<sub>2</sub> (Fachini et al., 2023). Some of the copper (II) crystal structures with 4-nitroimidazole derivatives have been mislabeled as 5-nitroimidazoles (Barba-Behrens et al., 1991; Atria et al., 2011; Fachini et al., 2023). All crystal structures coincide with a 4-nitroimidazole chelating coordination mode, via (N3)<sub>iz</sub> and

(O)NO<sub>2</sub>, to the metal center, presenting large Cu-NO<sub>2</sub> bond lengths (2.6–2.9 Å), (Figure 3). Fachini et al. have discussed the large nitro NO-metal bond lengths based on theoretical calculations of the Independent Gradient Model (IGM) and the Intrinsic Bond Strength Index (IBSI), and they conclude that the nitro NO-Cu bond (2.6–2.9 Å) has a weak bonding interaction, less than a quarter of the strength of the regular O-Cu bond (1.9–2.4 Å) (Fachini et al., 2023).

Oral diseases represent a major public health problem, ranking among the most prevalent conditions worldwide. These can significantly reduce patients' quality of life (Peres et al., 2019). The oral cavity hosts one of the most extensively studied microbiomes, enabling the identification of specific bacterial species associated with various diseases. For example, *Porphyromonas gingivalis*, *Treponema denticola*, and *Tannerella forsythia* are associated with periodontitis, while *Streptococcus mutans* and *Lactobacillus spp.* are associated with dental cavities (Krishnan et al., 2017; Willis and Gabaldón, 2020). Metronidazole has been used for the treatment of gingivitis since the 1990s. In recent years, due to the prevalence of these infections, novel smart bioactive materials have been developed that respond to chemical or physical stimuli (pH, enzymes, magnetism, electricity, and vibrations) to deliver antimicrobial agents such as chemical compounds (antibiotics), cationic monomers, antimicrobial peptides and metallic and non-metallic fillers (Montoya et al., 2023; Melo et al., 2025). However, metal-based drugs for the treatment of these infections have not been explored.

We have been interested in the development of metallo-drugs to broaden the spectrum of the biological action of nitroimidazole derivatives. Coordination compounds with biologically active ligands could re-emerge as a plausible treatment for infectious diseases (Turner, 2024). Recently, we obtained a series of copper (II) coordination compounds with 5-nitroimidazole derivatives, ornidazole (onz) and tinidazole (5tnz), [Cu(onz)<sub>2</sub>X<sub>2</sub>] and [Cu(5tnz)<sub>2</sub>X<sub>2</sub>]. These compounds have shown high antiparasitic activity against *T. gondii* and *Dactylogyrid monogeanis*, respectively, with low acute toxicity (Navarro-Peñaloza et al., 2026; Castro-Ramírez and Barba-Behrens, 2025). We investigated diverse

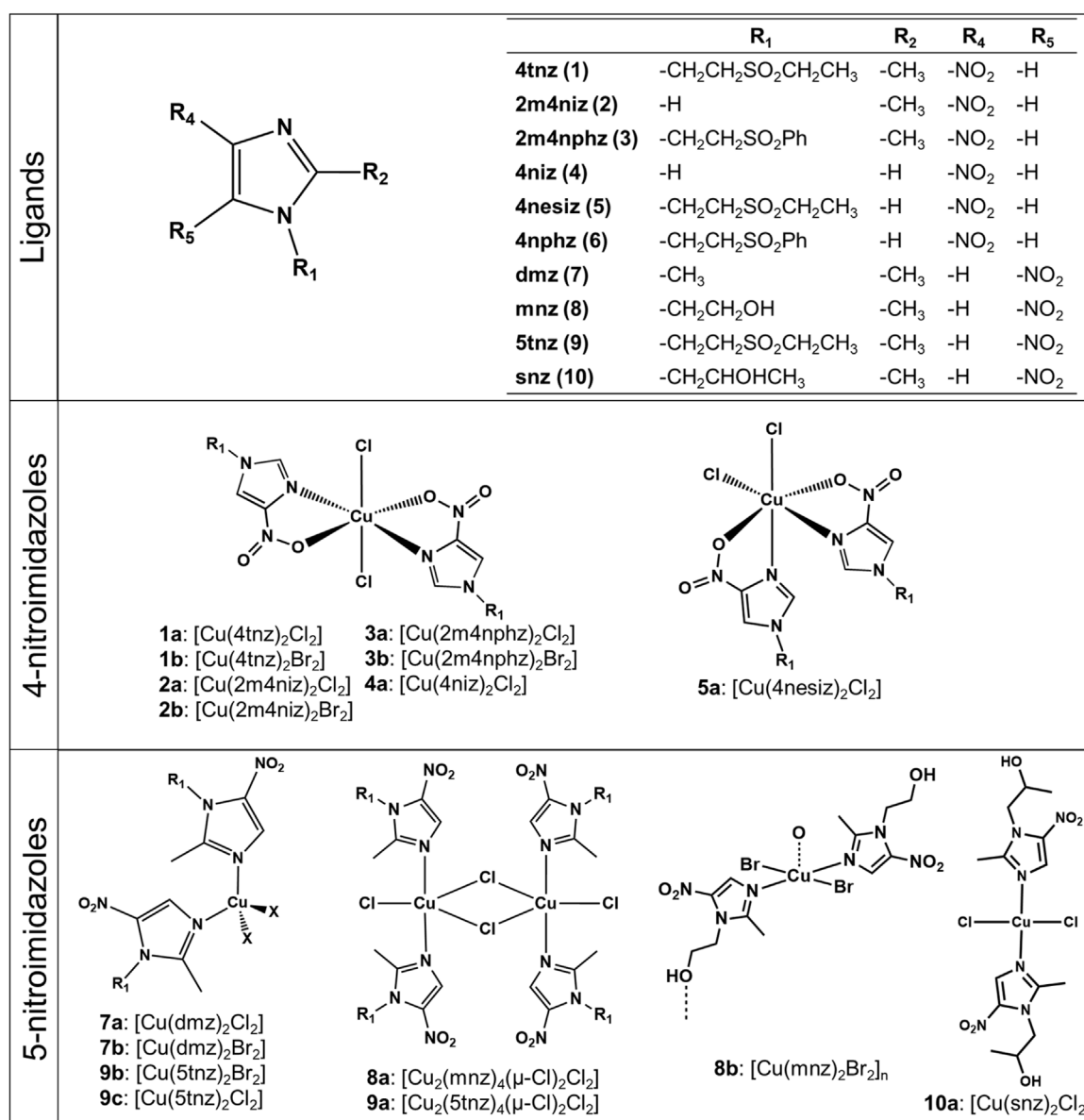


FIGURE 4  
Nitroimidazole ligands and their copper (II) coordination compounds studied in this work.

factors that could contribute to the biological activity of these complexes, such as the geometry of the metal ion, non-covalent interactions, redox behavior of the nitro group and metal ions, among others.

In this context, we decided to investigate 4- and 5-nitroimidazole derivatives to study their reactivity, stability, and coordination behavior toward copper (II) metal ions, driven by the different position of the nitro group in the imidazole heterocycle (Figure 4). Density functional theory (DFT) quantum chemical calculations were performed for a further understanding of their chemical and physicochemical properties. The use of the quantum theory of atoms in molecules has been useful in characterizing coordination compound interactions and stability (Cortés-Guzmán and Bader, 2005). Additionally, the biological activity of the 5-nitroimidazole coordination compounds was investigated to explore

their possible application for the treatment of periodontal and opportunistic bacteria.

## 2 Materials and methods

### 2.1 Chemical reagents

All reagents and solvents were used without further purification. Phenyl vinyl sulfone, ethyl vinyl sulfone, 2-methyl-4 (5)-nitroimidazole (2), 4-nitroimidazole (4), dimetridazole (7), metronidazole (8), and secnidazole (10) were obtained from Sigma-Aldrich; CuCl<sub>2</sub>·2H<sub>2</sub>O(a), CuBr<sub>2</sub>(b), and solvents were obtained from J.T. Baker; tinidazole (9) was obtained from Aarti Drugs Ltd.

## 2.2 Synthesis of the nitroimidazole ligands and their coordination compounds

### 2.2.1 4-Nitroimidazole derivatives

An isomerization reaction was used to synthesize 4tnz (**1**). An aza-Michael reaction was performed to synthesize 2m4nphz (**3**), 4nesiz (**5**), and 4nphz (**6**). Reactions were carried out in round-bottom flasks with a 30 mL aqueous solution of the reagents and 10% mol  $\text{HNaCO}_3$  under reflux for 24 h. The reaction solution was allowed to stand at room temperature for 1 h, and the solid product was collected via vacuum filtration, dried under vacuum, and used without further purification.

#### 2.2.1.1 Isomerization

4tnz: 1-(2-(ethylsulfonyl)ethyl)-2-methyl-4-nitroimidazole (**1**)

4tnz was synthesized via isomerization of tinidazole (**9**), as reported by Bhujanga Rao et al. (1989).

#### 2.2.1.2 Aza-michael reaction

2m4nphz: 2-methyl-4-nitro-1-(2-(phenylsulfonyl)ethyl)imidazole (**3**)

A white precipitate was obtained from 2-methyl-4 (5)-nitroimidazole (**2**) (474.1 mg; 3.7 mmol) and phenylvinylsulfone (565.1 mg; 3.4 mmol). Yield: 88%, 851.8 mg, 3.0 mmol. M.P.: 178–179 °C. Anal. (%) calc. for  $\text{C}_{12}\text{H}_{13}\text{N}_3\text{O}_4\text{S}$ : C, 48.81; H, 4.44; N, 14.23; and S, 10.86. Found: C, 48.56; H, 4.58; N, 13.75; and S, 10.60.  $^1\text{H}$  NMR (DMSO- $d_6$ , 400 MHz)  $\delta_{\text{H}}$  (ppm): 2.32 (s, 3H), 4.05 (t, 2H), 4.35 (t, 2H), 7.61 (t, 2H), 7.72 (t, 1H), 7.85 (d, 2H), and 8.17 (s, 1H).  $^{13}\text{C}\{^1\text{H}\}$  (DMSO- $d_6$ , 400 MHz)  $\delta_{\text{C}}$  (ppm): 12.99, 40.87, 53.84, 122.51, 127.77, 129.91, 134.47, 139.29, 145.54, and 145.78.

4nesiz: 1-(2-(ethylsulfonyl)ethyl)-4-nitroimidazole (**5**)

A white precipitate was obtained from 4-nitroimidazole (**4**) (540.7 mg; 4.8 mmol) and ethylvinylsulfone (0.5 mL; 4.8 mmol). Yield: 55%, 618.6 mg, 2.7 mmol. M.P.: 98–100 °C. Anal. (%) calc. for  $\text{C}_7\text{H}_{11}\text{N}_3\text{O}_4\text{S}$ : C, 36.05; H, 4.75; N, 18.02; and S, 13.75. Found: C, 36.09; H, 4.86; N, 18.52; and S, 13.56.  $^1\text{H}$  NMR (DMSO- $d_6$ , 400 MHz)  $\delta_{\text{H}}$  (ppm): 1.19 (t, 3H), 3.10 (q, 2H), 3.73 (t, 2H), 4.50 (t, 2H), 7.88 (d, 1H), and 8.45 (d, 1H).  $^{13}\text{C}\{^1\text{H}\}$  (DMSO- $d_6$ , 400 MHz)  $\delta_{\text{C}}$  (ppm): 6.53, 41.34, 47.53, 50.99, 122.35, 138.32, and 147.48.

4nphz: 1-(2-(phenylsulfonyl)ethyl)-4-nitroimidazole (**6**)

A white precipitate was obtained from 4-nitroimidazole (**4**) (446.5 mg; 4.0 mmol) and phenylvinylsulfone (595.6 mg; 3.5 mmol). Yield: 80%, 800.9 mg, 2.8 mmol. M.P.: 168–170 °C. Anal. (%) calc. for  $\text{C}_{11}\text{H}_{11}\text{N}_3\text{O}_4\text{S}$ : C, 46.97; H, 3.94; N, 14.94; and S, 11.40. Found: C, 46.72; H, 3.90; N, 15.21; and S, 10.83.  $^1\text{H}$  NMR (DMSO- $d_6$ , 400 MHz)  $\delta_{\text{H}}$  (ppm): 4.08 (t, 2H), 4.45 (t, 2H), 7.61 (t, 2H), 7.72 (t, 1H), 7.84 (d, 3H), and 8.33 (d, 1H).  $^{13}\text{C}\{^1\text{H}\}$  (DMSO- $d_6$ , 400 MHz)  $\delta_{\text{C}}$  (ppm): 41.98, 54.17, 122.07, 127.93, 129.92, 134.48, 138.13, 139.23, and 147.32.

### 2.2.2 Copper (II) coordination compounds

Compounds  $[\text{Cu}_2(\text{mnz})_4\text{Cl}_2(\mu\text{-Cl})_2]$  (**8a**),  $[\text{Cu}_2(5\text{tnz})_4\text{Cl}_2(\mu\text{-Cl})_2]$  (**9a**), and  $[\text{Cu}(5\text{tnz})_2\text{Br}_2]$  (**9b**) were synthesized, as previously reported (Barba-Behrens et al., 1991; Alfaro-Fuentes et al., 2014). The remaining coordination compounds were synthesized as follows, unless stated otherwise: a 20 mL methanolic solution of the corresponding nitroimidazole and copper (II) salt was heated in a round-bottom flask under reflux conditions for 2 h. The resulting

solution was allowed to reach room temperature for the reaction product to precipitate. The resulting product was collected via suction filtration, dried in a vacuum, and used without further purification.

#### 2.2.2.1 4-Nitroimidazole coordination compounds

$[\text{Cu}(4\text{tnz})_2\text{Cl}_2]$  (**1a**)

A blue precipitate was obtained from  $\text{CuCl}_2 \cdot 2\text{H}_2\text{O}$  (279.3 mg; 1.6 mmol) and 4tnz (**1**) (794.2 mg; 3.2 mmol). Yield: 85%, 851.8 mg, 1.2 mmol. Blue crystals suitable for X-ray analysis were obtained by slow evaporation at room temperature from the reaction solution. Anal. (%) calc. for  $\text{C}_{16}\text{H}_{26}\text{Cl}_2\text{CuN}_6\text{O}_8\text{S}_2$ : C, 30.55; H, 4.17; N, 13.36; and S, 10.20. Found: C, 30.50; H, 4.19; N, 13.49; S, 10.04.

$[\text{Cu}(4\text{tnz})_2\text{Br}_2]$  (**1b**)

An olive-green precipitate was obtained from  $\text{CuBr}_2$  (316.3 mg; 1.4 mmol) and 4tnz (**1**) (693.4 mg; 2.8 mmol). Yield: 93%, 928.6 mg, 1.3 mmol. Anal. (%) calc. for  $\text{C}_{16}\text{H}_{26}\text{Br}_2\text{CuN}_6\text{O}_8\text{S}_2$  (%): C, 26.77; H, 3.65; N, 11.71; and S, 8.93. Found: C, 26.66; H, 3.76; N, 11.93; and S, 8.72.

$[\text{Cu}(2\text{m4niz})_2\text{Cl}_2]$  (**2a**)

A blue precipitate was obtained from  $\text{CuCl}_2 \cdot 2\text{H}_2\text{O}$  (438.6 mg; 2.6 mmol) and 2m4niz (**2**) (647.7 mg; 5.1 mmol). Yield 78%, 820.1 mg, 2.1 mmol. Anal. (%) Calc. for  $\text{C}_8\text{H}_{10}\text{Cl}_2\text{CuN}_6\text{O}_4$  (%): C 24.72, H 2.59, N 21.62. Found: C 24.90, H 2.56, N 21.60. The reaction solution was left to stand at room temperature for a week, and blue crystals suitable for X-ray analysis were obtained by slow evaporation.

$[\text{Cu}(2\text{m4niz})_2\text{Br}_2]$  (**2b**)

A deep-green precipitate was obtained from  $\text{CuBr}_2$  (468.8 mg; 2.1 mmol) and 2m4niz (**2**) (552.6 mg; 4.2 mmol). Yield: 80%, 791.6 mg, 1.6 mmol. Dark green crystals suitable for X-ray analysis were obtained by slow evaporation at room temperature from the reaction solution. Anal. (%) Calc. for  $\text{C}_8\text{H}_{10}\text{Br}_2\text{CuN}_6\text{O}_4$  (%): C, 20.12; H, 2.11; and N, 17.60. Found: C, 19.14; H, 2.68; and N, 16.62.

$[\text{Cu}(2\text{m4nphz})_2\text{Cl}_2]$  (**3a**)

A blue precipitate was obtained from  $\text{CuCl}_2 \cdot 2\text{H}_2\text{O}$  (43.5 mg; 0.25 mmol) and 2m4nphz (**3**) (147.2 mg; 0.5 mmol). Yield: 91%, 164.5 mg, 0.23 mmol. Anal. (%) calc. for  $\text{C}_{24}\text{H}_{26}\text{Cl}_2\text{CuN}_6\text{O}_8\text{S}_2$  (%): C, 39.76; H, 3.61; N, 11.59; and S, 8.84. Found: C, 39.69; H, 3.88; N, 11.37; and S, 8.52.

$[\text{Cu}(2\text{m4nphz})_2\text{Br}_2]$  (**3b**)

A deep-green precipitate was obtained from  $\text{CuBr}_2$  (57.8 mg; 0.25 mmol) and 2m4nphz (**3**) (148.0 mg; 0.5 mmol). Yield 86%, 175.1 mg, 0.22 mmol. Anal. (%) calc. for  $\text{C}_{24}\text{H}_{26}\text{Br}_2\text{CuN}_6\text{O}_8\text{S}_2$  (%): C, 35.41; H, 3.22; N, 10.32; and S, 7.88. Found: C, 35.35; H, 3.45; N, 10.10; and S, 7.50.

### [Cu(4niz)<sub>2</sub>Cl<sub>2</sub>] (4a)

A blue precipitate was obtained from CuCl<sub>2</sub>·2H<sub>2</sub>O (171.7 mg; 1.0 mmol) and 4niz (4) (115.0 mg; 1.0 mmol). Yield: 53%, 96.1 mg, 0.26 mmol. The green reaction solution was allowed to evaporate at room temperature to form blue crystals suitable for X-ray diffraction. Anal. (%) calc. for C<sub>6</sub>H<sub>6</sub>Cl<sub>2</sub>CuN<sub>6</sub>O<sub>4</sub> (%): C, 19.98; H, 1.68; and N, 23.31. Found: C, 19.94; H, 1.56; and N, 23.21.

### [Cu(4nesiz)<sub>2</sub>Cl<sub>2</sub>] (5a)

A green solution of CuCl<sub>2</sub>·2H<sub>2</sub>O (42.6 mg; 0.25 mmol) and 4nesiz (5) (116.7 mg; 0.5 mmol) was allowed to evaporate at room temperature, yielding blue crystals suitable for X-ray diffraction. Anal. (%) calc. for C<sub>14</sub>H<sub>22</sub>Cl<sub>2</sub>CuN<sub>6</sub>O<sub>8</sub>S<sub>2</sub> (%): C, 27.98; H, 3.69; N, 13.98; and S, 10.67. Found: C, 28.01; H, 3.69; N, 14.12; and S, 10.58.

#### 2.2.2.2 5-Nitroimidazole copper (II) coordination compounds

### [Cu(dmz)<sub>2</sub>Cl<sub>2</sub>] (7a)

A green precipitate was obtained from CuCl<sub>2</sub>·2H<sub>2</sub>O (196.1 mg; 1.2 mmol) and dmz (7) (324.6 mg; 2.3 mmol). Yield: 75%, 403.6 mg, 0.9 mmol. Green crystals suitable for X-ray analysis were obtained by slow evaporation at room temperature from the reaction solution. Anal. (%) calc. for C<sub>10</sub>H<sub>14</sub>Cl<sub>2</sub>CuN<sub>6</sub>O<sub>4</sub>: C, 28.82; H, 3.39; and N, 20.17. Found: C, 28.73; H, 3.40; and N, 19.90.

### [Cu(dmz)<sub>2</sub>Br<sub>2</sub>] (7b)

A red-brownish precipitate was obtained from CuBr<sub>2</sub> (447.2 mg; 2.0 mmol) and dmz (7) (559.7 mg; 4.0 mmol). Yield: 81%, 813.5 mg, 1.6 mmol. Dark red crystals suitable for X-ray analysis were obtained by slow evaporation at room temperature from the reaction solution. Anal. (%) calc. for C<sub>10</sub>H<sub>14</sub>Br<sub>2</sub>CuN<sub>6</sub>O<sub>4</sub>: C, 23.75; H, 2.79; and N, 16.62. Found: C, 23.75; H, 2.81; and N, 16.44.

### [Cu(mnz)<sub>2</sub>Br<sub>2</sub>]<sub>n</sub> (8b)

A deep-green precipitate was obtained from CuBr<sub>2</sub> (202.7 mg, 0.9 mmol) and mnz (8) (302.7 mg, 1.8 mmol). Yield: 75%, 375.6 mg, 0.66 mmol. Green crystals suitable for X-ray analysis were obtained by slow evaporation at room temperature from the solution. Anal. (%) calc. for C<sub>12</sub>H<sub>18</sub>Br<sub>2</sub>CuN<sub>6</sub>O<sub>6</sub>: C, 25.48; H, 3.21; and N, 14.86. Found: C, 25.52; H, 3.21; and N, 14.65.

### [Cu(snz)<sub>2</sub>Cl<sub>2</sub>] (10a)

A 20 mL ethanolic solution of copper (II) chloride hemihydrate (37.0 mg, 0.2 mmol) and a racemic mixture of secnidazole (10) (17.1 mg, 0.1 mmol) was added to a 23 mL Teflon-lined reactor and then placed into a stainless steel autoclave (Parr Instruments). The autoclave was sealed, and the reaction mixture was heated to 85 °C and maintained at this temperature for 12 h. At the end of the reaction, the autoclave was set to cool for 36 h. Purple crystals suitable for X-ray diffraction were collected. Anal. (%) calc. for C<sub>14</sub>H<sub>22</sub>Cl<sub>2</sub>CuN<sub>6</sub>O<sub>6</sub>: C, 33.31; H, 4.39; and N, 16.65. Found: C, 33.26; H, 4.41; and N, 16.40.

## 2.3 Physical measurements

Fourier-transform infrared (FT-IR) and far-infrared (FIR) spectra were recorded with an FT-IR/FT-FIR spectrum 400 spectrophotometer using a universal attenuated total reflectance (ATR) accessory from Perkin-Elmer (4000–400 cm<sup>-1</sup>). The UV-Vis-NIR spectra (diffuse reflectance, 40,000–5000 cm<sup>-1</sup>) were recorded on a Cary-5000 (Varian) spectrophotometer. Elemental analyses were carried out with a Fisons EA 1180 analyzer. NMR spectra were obtained in a Varian Unity Inova spectrometer with a frequency of 400 MHz for <sup>1</sup>H and 100 MHz for <sup>13</sup>C, using DMSO-d<sub>6</sub> as solvent. Chemical shifts (δ) are reported in ppm in reference to tetramethylsilane (TMS). Electron paramagnetic resonance (EPR) spectra were measured under non-saturating microwave power conditions on a Bruker Elexsys E500 instrument in solid state at room temperature (X-band, 100 kHz modulation).

X-ray diffraction data were obtained using standard procedures on an Oxford Diffraction Gemini “A” instrument with a CCD area detector using graphite-monochromated Mo Kα radiation at 130 K. Intensities were measured using φ + ω scans. All structures were solved using direct methods, using SHELX-972, and the refinement (based on *F*<sup>2</sup> of all data) was performed by the full-matrix least-squares techniques with Crystals v. 12.84 software (Sheldrick, 2008). All non-hydrogen atoms were refined anisotropically, and all hydrogen atoms attached to C atoms were positioned geometrically as riding on their parent atoms, with C–H = 0.93–0.99 Å and Uiso(H) = –1.2Ueq(C) for aromatic and methylene groups and Uiso(H) = –1.5Ueq(C) for methyl groups (Clark and Reid, 1995; Hübschle et al., 2011). Crystallographic tables can be found in Supplementary Tables S1, S2. The crystallographic data for the structures have been deposited at the Cambridge Crystallographic Data Centre as supplementary publication CCDC 2498924–2498933 and 2499210. Copies of the data can be obtained free of charge via [www.ccdc.cam.ac.uk/data\\_request/cif](http://www.ccdc.cam.ac.uk/data_request/cif).

## 2.4 Computational methods

In order to understand the water stability of the copper coordination compounds of 4tnz, the 4tnz and 5tnz ligands and the [Cu(4tnz)<sub>2</sub>Cl<sub>2</sub>] (1a) and [Cu(5tnz)<sub>2</sub>Cl<sub>2</sub>] (9c) complexes were studied by DFT calculations at the PBE0/def2-TZVP level of theory, using the Grimme D3(BJ) scheme for dispersion corrections (Grimme et al., 2011) and the implicit solvent SMD method (Marenich et al., 2009) for water effects. In all cases, full geometry optimization was performed, followed by vibrational analysis, to corroborate that these structures correspond to minima on the potential energy surface. The initial X-ray diffraction structure of [Cu(4tnz)<sub>2</sub>Cl<sub>2</sub>] (1a) is from this work, and that of [Cu(5tnz)<sub>2</sub>Cl<sub>2</sub>] (9c) is taken from a previously reported structure (Alfaro-Fuentes et al., 2014). The energetic contributions of the imidazole ring, the methyl, the nitro, and the (ethylsulfonyl)ethyl groups to the total stability of the ligands and complexes were analyzed through the corresponding atomic energies calculated within the Quantum Theory of Atoms in Molecules (QTAIM) methodology (Bader and Nguyen-Dang, 1981). The nature and strength of the coordination bonds

formed between the two ligands and the Cu<sup>2+</sup> ion were examined by the QTAIM and the Non-Covalent Interaction (NCI) index frameworks (Johnson et al., 2010). Moreover, the water stability of [Cu(4tnz)<sub>2</sub>Cl<sub>2</sub>] (**1a**) and [Cu(5tnz)<sub>2</sub>Cl<sub>2</sub>] (**9c**) was also tested by the addition of two water molecules, close to the metallic center of each complex. The geometries of the corresponding models, [Cu(4tnz)<sub>2</sub>Cl<sub>2</sub>]•2H<sub>2</sub>O and [Cu(5tnz)<sub>2</sub>Cl<sub>2</sub>]•2H<sub>2</sub>O, were also relaxed using the same methodology. All the DFT calculations were performed using Gaussian 16 software (Frisch et al., 2016). The QTAIM and NCI analyses were carried out with the AIMALL and NCIPlot4 programs (Version 17.11.14) (Todd and Gristmill, 2019; Boto et al., 2020).

## 2.5 Biological assays

### 2.5.1 Antimicrobial studies

Two oral bacteria and two aerobic opportunistic bacteria were acquired from the American Type Culture Collection (ATCC) for the antibacterial tests shown in Table 1. The opportunistic strains were individually cultured on agar plates with Trypticase Soy Agar (TSA) (BBL, Becton-Dickinson) and incubated for 24 h at 37 °C under aerobic conditions. The anaerobic oral bacteria were individually cultured on enriched agar plates with *Mycoplasma* (Sigma-Aldrich) and 5% defibrinated lamb blood (Microlab), and incubated for 7 days at 35 °C under anaerobic conditions (80% N<sub>2</sub>, 10% CO<sub>2</sub>, and 10% H<sub>2</sub>). Pure cultures of each strain were used in the experiments. After the incubation period, the individual cultures were collected and resuspended in culture media, TSB broth, or enriched *Mycoplasma* broth (BBL, Becton-Dickinson), supplemented with 5 µg/mL hemin and 0.3 µg/mL menadione, depending on the strain. The optical density (OD) in each bacterial suspension was adjusted to 1 at λ = 600 nm in a spectrophotometer (BioPhotometer D30, Eppendorf) to obtain a bacterial suspension with 10<sup>9</sup> cells/mL.

The antimicrobial susceptibilities of the ligands 7–9 and their copper (II) coordination compounds were determined using the minimum bactericidal concentration (MBC) experiment based on the Clinical and Laboratory Standards Institute (CLSI) (Paz-Diaz et al., 2023; Reyes-Carmona et al., 2023).

#### 2.5.1.1 Minimum bacterial concentration

The MBCs were determined by the microdilution method in broth culture in 96-well plates. An aqueous solution of each coordination compound was prepared and sterilized at a concentration of 3 × 10<sup>-2</sup> M. Concentrations ranged from 3 × 10<sup>-3</sup> M to 1.2 × 10<sup>-5</sup> M per copper atom. Each well was aseptically inoculated with 20 µL of a bacterial suspension at a concentration of 10<sup>5</sup> bacteria/mL. Chlorhexidine (2%) was used as the positive control, and sterile medium was used as the negative control. The 96-well plates were incubated for 24 h at 35 °C in aerobic or anaerobic conditions. After the incubation period, 5 µL of bacterial suspension from the wells was transferred to agar plates with TSA or *Mycoplasma* agar with 5% defibrinated sheep blood, depending on the bacteria, and incubated under the conditions specified above. The experiments were performed in duplicate.

TABLE 1 Selected bacteria for antibacterial tests organized by oxygen requirement, cell wall composition, and pathological relevance.

Oxygen requirement	Gram-positive	Gram-negative	Pathogen
Aerobic	<i>Staphylococcus aureus</i> (ATCC 25923)	<i>Escherichia coli</i> (ATCC 33780)	Opportunistic
Anaerobic	<i>Streptococcus mutans</i> (ATCC 25175)	<i>Porphyromonas gingivalis</i> (ATCC 33277)	Oral

## 3 Results and discussion

In order to investigate the differences on the coordination properties of 4- and 5-nitroimidazole derivatives toward copper (II), a series of nitroimidazole coordination compounds was synthesized and fully characterized by elemental analysis, FT-IR, FIR, EPR, and electronic absorption spectroscopy, and by single crystal X-ray diffraction of compounds 4tnz (**1**), 2m4nphz (**3**), [Cu(4tnz)<sub>2</sub>Cl<sub>2</sub>] (**1a**), [Cu(2m4niz)<sub>2</sub>Cl<sub>2</sub>] (**2a**), [Cu(2m4niz)<sub>2</sub>Br<sub>2</sub>] (**2b**), [Cu(4niz)<sub>2</sub>Cl<sub>2</sub>] (**4a**), [Cu(4nesiz)<sub>2</sub>Cl<sub>2</sub>] (**5a**), [Cu(dmz)<sub>2</sub>Cl<sub>2</sub>] (**7a**), [Cu(dmz)<sub>2</sub>Br<sub>2</sub>] (**7b**), [Cu(mnz)<sub>2</sub>Br<sub>2</sub>]<sub>n</sub> (**8b**), and [Cu(snz)<sub>2</sub>Cl<sub>2</sub>] (**10a**).

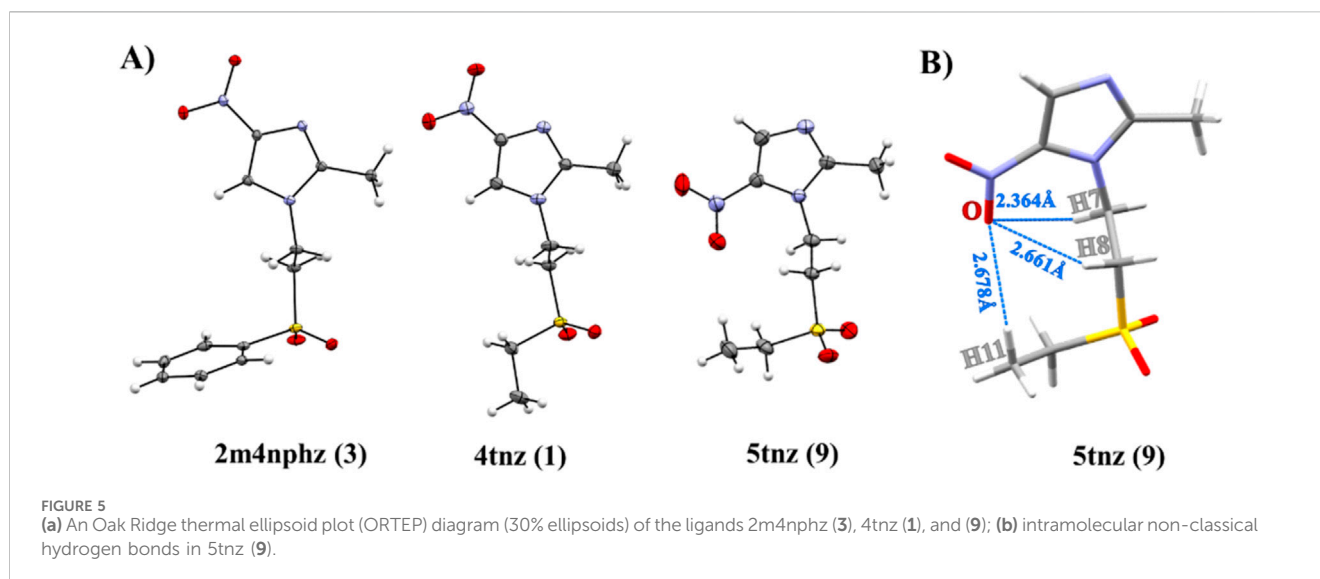
### 3.1 Characterization in solid state and solution

#### 3.1.1 4-Nitroimidazole coordination compounds

##### 3.1.1.1 Infrared spectroscopy

The 4-nitroimidazole ligands and their coordination compounds presented characteristic vibration bands of nitroimidazole: ν(C=N) 1537–1545 cm<sup>-1</sup>, ν<sub>as</sub> (NO<sub>2</sub>) 1487–1508 cm<sup>-1</sup>, and ν<sub>s</sub> (NO<sub>2</sub>) 1373–1399 cm<sup>-1</sup> (Arjunan et al., 2012). These bands shifted to higher energy upon a chelate coordination to the metal ion, N3 from the imidazole ring, and an O atom from the nitro group (Supplementary Table S3).

Previous work observed that the 5tnz coordination compounds may present lone pair S-O:⋯π non-covalent interactions. In these complexes, an oxygen of the sulfone group presented an intramolecular lone pair S-O:⋯π<sub>iz</sub> interaction with the imidazole ring (Alfaro-Fuentes et al., 2014). On their IR spectra, shifting of the bands ν<sub>as</sub> (SO<sub>2</sub>) 1290–1305 cm<sup>-1</sup> and ν<sub>s</sub> (SO<sub>2</sub>) 1120–1130 cm<sup>-1</sup> was observed, which was characteristic of this type of lone pair⋯π<sub>iz</sub> interaction. A similar shift was observed for [Cu(4nesiz)<sub>2</sub>Cl<sub>2</sub>] (**5a**), ν<sub>as</sub> (SO<sub>2</sub>) 1291 cm<sup>-1</sup> and ν<sub>s</sub> (SO<sub>2</sub>) 1121 cm<sup>-1</sup>. These sulfone oxygens may also present intermolecular interactions, lone pair S-O:⋯π-(hole)NO<sub>2</sub>, with a neighboring nitro group (Ramírez-Palma et al., 2023), ν<sub>as</sub> (SO<sub>2</sub>) 1300 cm<sup>-1</sup> and ν<sub>s</sub> (SO<sub>2</sub>) 1130 cm<sup>-1</sup>. For the [Cu(4tnz)<sub>2</sub>Cl<sub>2</sub>] (**1a**) and [Cu(4tnz)<sub>2</sub>Br<sub>2</sub>] (**1b**) complexes, these bands were observed at ν<sub>as</sub> (SO<sub>2</sub>) 1303 cm<sup>-1</sup> and ν<sub>s</sub> (SO<sub>2</sub>) 1124 cm<sup>-1</sup>. X-ray crystal structures confirmed the presence of a lone pair S-O:⋯π-(hole)NO<sub>2</sub> for compound **1a**, whereas compound **5a** stabilized a lone pair S-O:⋯π<sub>iz</sub>



interaction. Compounds with the ligand 2m4nphz do not present this type of interaction in their IR and their crystal structures (Flores-Leyva, 2018).

Additionally, the FIR spectra showed the expected vibration bands:  $\nu(\text{Cu-Cl})$  300–287  $\text{cm}^{-1}$ ,  $\nu(\text{Cu-Br})$  211–232  $\text{cm}^{-1}$ , and  $\nu(\text{Cu-O})$  288–299  $\text{cm}^{-1}$ . These bands correspond to an  $\nu(\text{Cu-X})$  in an octahedral geometry for the metal center (Clark and Williams, 1964).

### 3.1.1.2 Electronic spectroscopy

Reflectance spectra for the 4-nitroimidazole-copper (II) coordination compounds showed a d-d transition centered at ca. 14,200  $\text{cm}^{-1}$  with a shoulder at ca. 16,400  $\text{cm}^{-1}$ , characteristic of a rhombic distorted octahedral copper (II) compound (Supplementary Figure S1, Supplementary Table S4). Solution electronic spectra of coordination compounds and copper (II) salts were obtained in DMSO, EtOH, MeCN, and aqueous solution. The compounds presented a single d-d transition centered at 945 nm (DMSO), 880 nm (EtOH), 840 nm (MeCN), and 800 nm ( $\text{H}_2\text{O}$ ), indicating that the 4-nitroimidazole coordination compounds dissociated to a similar copper (II) species in solution, which was not expected for chelating bidentate ligands (Supplementary Table S4).

### 3.1.1.3 X-ray studies

The crystal structures of the 4-nitroimidazole derivatives 1-(2-(ethylsulfonyl)ethyl)-2-methyl-4-nitroimidazole (4tnz) and 2-methyl-4-nitro-1-(2-(phenylsulfonyl)ethyl)imidazole (2m4nphz) showed that by changing the position of the nitro group, the N-substituted side chains (N-ethylsulfone and N-phenylsulfone) are not able to present intramolecular interactions with the  $\text{NO}_2$ , as was observed for the isomer 5tnz, where the orientation of the nitro group gives place to three non-classical hydrogen bonds ( $\text{O} \cdots \text{H7C7}$ : 2.364 Å,  $\text{O} \cdots \text{H8C8}$ : 2.661 Å,  $\text{O} \cdots \text{H11C11}$ : 2.678 Å) (Desiraju and Steiner, 2001; Salazar-Cano et al., 2016; Varga et al., 2024; Figure 5).

The structures of the copper (II) coordination compounds  $[\text{Cu}(4\text{tnz})_2\text{Cl}_2]$  (**1a**),  $[\text{Cu}(2\text{m4niz})_2\text{Cl}_2]$  (**2a**),  $[\text{Cu}(2\text{m4niz})_2\text{Br}_2]$  (**2b**),

and  $[\text{Cu}(4\text{niz})_2\text{Cl}_2]$  (**4a**) were obtained by X-ray diffraction. In all complexes, two 4-nitroimidazole ligands were coordinated to the copper (II) center as a bidentate ligand through the N3 of the imidazole ring, Cu-N (1.967–1.993 Å), and an O from the nitro group, Cu-O (2.558–2.649 Å), in an all *trans*-octahedral geometry (Figure 6). The bond lengths are included in Supplementary Table S6 in Supplementary Material. The complexes with 2-methyl derivatives present intramolecular non-classical hydrogen bonds between an O from the nitro group and a hydrogen from the methyl group. It is noteworthy that the absence of the 2-methyl group in the sulfone derivative,  $[\text{Cu}(4\text{nesiz})_2\text{Cl}_2]$  (**5a**), gives place to a *cis*-octahedral geometry, which presented the longest bond distances (Cu-N: 2.019 Å and Cu-O: 2.746 Å; Figure 6). In the electronic spectrum, the d-d transition is shifted to lower energy (13,000  $\text{cm}^{-1}$ ), compared with the *trans*-octahedral (ca. 15,300  $\text{cm}^{-1}$ ), indicative of a weaker crystal field splitting, and the  $\nu(\text{Cu-Cl})$  band in the FIR is shifted to higher energy (314  $\text{cm}^{-1}$ ). The spectroscopic and analytical characterization of compound **2a** was from the solid compound isolated from the reaction mixture. Crystals were obtained from this MeOH solution after a week. The copper (II) compound **2a** crystallized with methanol as co-solvent,  $[\text{Cu}(2\text{m4niz})_2\text{Cl}_2] \cdot \text{MeOH}$ .

The *trans*-octahedral compounds  $[\text{Cu}(2\text{m4niz})_2\text{Cl}_2] \cdot \text{MeOH}$  (**2a**),  $[\text{Cu}(2\text{m4niz})_2\text{Br}_2]$  (**2b**), and  $[\text{Cu}(4\text{niz})_2\text{Cl}_2]$  (**4a**) presented similar parallel displaced  $\pi$ -stacking intermolecular interactions between the imidazole rings, due to the absence of substituents in the N1 position of the imidazole ring. In the case of the methylated *trans*- $[\text{Cu}(4\text{tnz})_2\text{Cl}_2]$  (**1a**), the extended conformation allowed both ligands to stabilize intermolecular lone pair S-O $\cdots\pi$ -(hole) $\text{NO}_2$  interactions, as shown in Figure 7a.

On the other hand, the absence of the 2-methyl group in the *cis*- $[\text{Cu}(4\text{nesiz})_2\text{Cl}_2]$  (**5a**) compound favors an intramolecular lone pair S-O $\cdots\pi_{\text{iz}}$ , being the only complex of the 4-nitroimidazole derivatives that presented this type of intramolecular interaction. A similar intramolecular lone pair S-O $\cdots\pi_{\text{iz}}$  interaction was observed in the biologically active  $[\text{Cu}(5\text{tnz})_2\text{Cl}_2]$  (**9c**) (Castro-Ramírez and Barba-Behrens, 2025; Figure 7b).

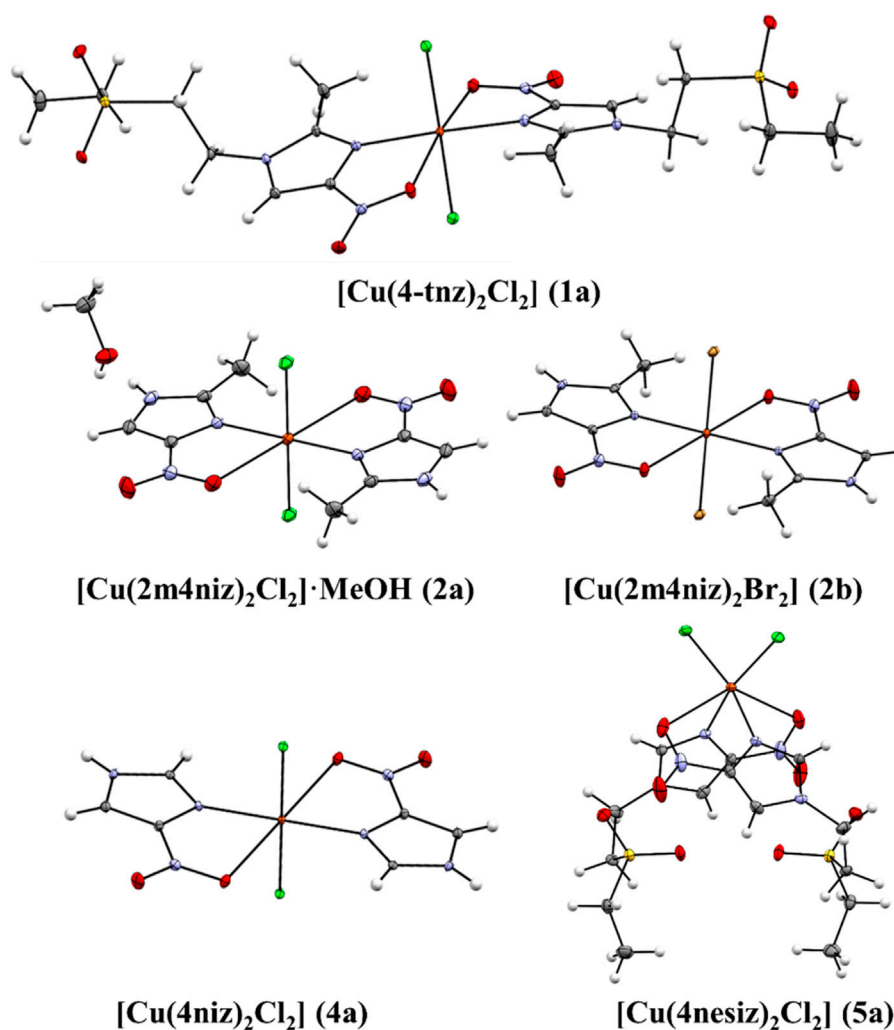


**FIGURE 6**  
ORTEP diagram (30% ellipsoids) of coordination compounds [Cu(4tnz)<sub>2</sub>Cl<sub>2</sub>] (1a), [Cu(2m4niz)<sub>2</sub>Cl<sub>2</sub>]·MeOH (2a), [Cu(2m4niz)<sub>2</sub>Br<sub>2</sub>] (2b), [Cu(4niz)<sub>2</sub>Cl<sub>2</sub>] (4a), and [Cu(4nesiz)<sub>2</sub>Cl<sub>2</sub>] (5a).

### 3.1.1.4 X-band EPR spectroscopy

EPR spectra of the *trans*-octahedral [Cu(4tnz)<sub>2</sub>Cl<sub>2</sub>] (1a), [Cu(4tnz)<sub>2</sub>Br<sub>2</sub>] (1b), [Cu(2m4niz)<sub>2</sub>Cl<sub>2</sub>] (2a), [Cu(2m4niz)<sub>2</sub>Br<sub>2</sub>] (2b), and [Cu(4niz)<sub>2</sub>Cl<sub>2</sub>] (4a) were obtained at room temperature. The spectra were typical of  $S = 1/2$  and  $I = 3/2$  copper species with axial symmetry on 1b and rhombic symmetry on 1a, 2a, 2b, and 4a (Supplementary Figure S2). The  $g$ -tensor values vary depending on the coordinated halogen. On the chloro complexes, the  $g_z$ ,  $g_y$ , and  $g_x$  values increased as the Cu-Cl bond length increased (Table 2). On the other hand, all the 5-nitroimidazole complexes showed typical  $S = 1/2$  and  $I = 3/2$  copper species with axial symmetry (Supplementary Figure S2). The  $g$ -tensor values vary depending on the geometry of the copper (II) atom, as noted in Table 2. As complexes presented different geometries: tetrahedral in [Cu(dmz)<sub>2</sub>Cl<sub>2</sub>] (7a) and [Cu(tnz)<sub>2</sub>Br<sub>2</sub>] (9b), square planar for [Cu(snz)<sub>2</sub>Cl<sub>2</sub>] (10a), squared based pyramidal (SBP) in the polymeric [Cu(mnz)<sub>2</sub>Br<sub>2</sub>]<sub>n</sub> (8b) and the dinuclear [Cu<sub>2</sub>(tnz)<sub>4</sub>(μ-Cl)<sub>2</sub>Cl<sub>2</sub>] (9a) compounds, and a trigonal bipyramidal (TBP) in [Cu<sub>2</sub>(mnz)<sub>4</sub>(μ-Cl)<sub>2</sub>Cl<sub>2</sub>] (8a).

### 3.1.2 5-Nitroimidazole coordination compounds

#### 3.1.2.1 Infrared spectroscopy

The characteristic vibration bands  $\nu(\text{C}=\text{N})$  1,523–1,535  $\text{cm}^{-1}$ ,  $\nu(\text{NO}_2)_{\text{as}}$  1,451–1,471  $\text{cm}^{-1}$ , and  $\nu(\text{NO}_2)_s$  1,354–1,367  $\text{cm}^{-1}$  were observed in the 5-nitroimidazole derivatives. In the copper (II) coordination compounds, the  $\nu(\text{C}=\text{N})$  band was shifted to higher energy, 1,551–1,559  $\text{cm}^{-1}$ , as did the uncoordinated nitro group  $\nu_{\text{as}}(\text{NO}_2)$  1,469–1,483  $\text{cm}^{-1}$ . In those ligands that present an alcohol group in the alkyl substituent, mnz (8) and snz (10), the  $\nu(\text{O}-\text{H})$  band shifted from 3,200  $\text{cm}^{-1}$ , in the free ligands, to 3,400  $\text{cm}^{-1}$  upon coordination to the metal ion due to the loss of the intermolecular hydrogen bonding between the OH and the N3 nitrogen from a neighboring imidazole, as seen in the reported crystal structure (Blaton et al., 1979). For compound [Cu(mnz)<sub>2</sub>Br<sub>2</sub>]<sub>n</sub> (8b), the  $\nu(\text{O}-\text{H})$  band was split into two bands, one corresponding to a coordinated alcohol group in 3,354  $\text{cm}^{-1}$  and the second to a free alcohol group in 3,410  $\text{cm}^{-1}$ , as was observed in its crystal structure (Supplementary Table S5, Supplementary Material).

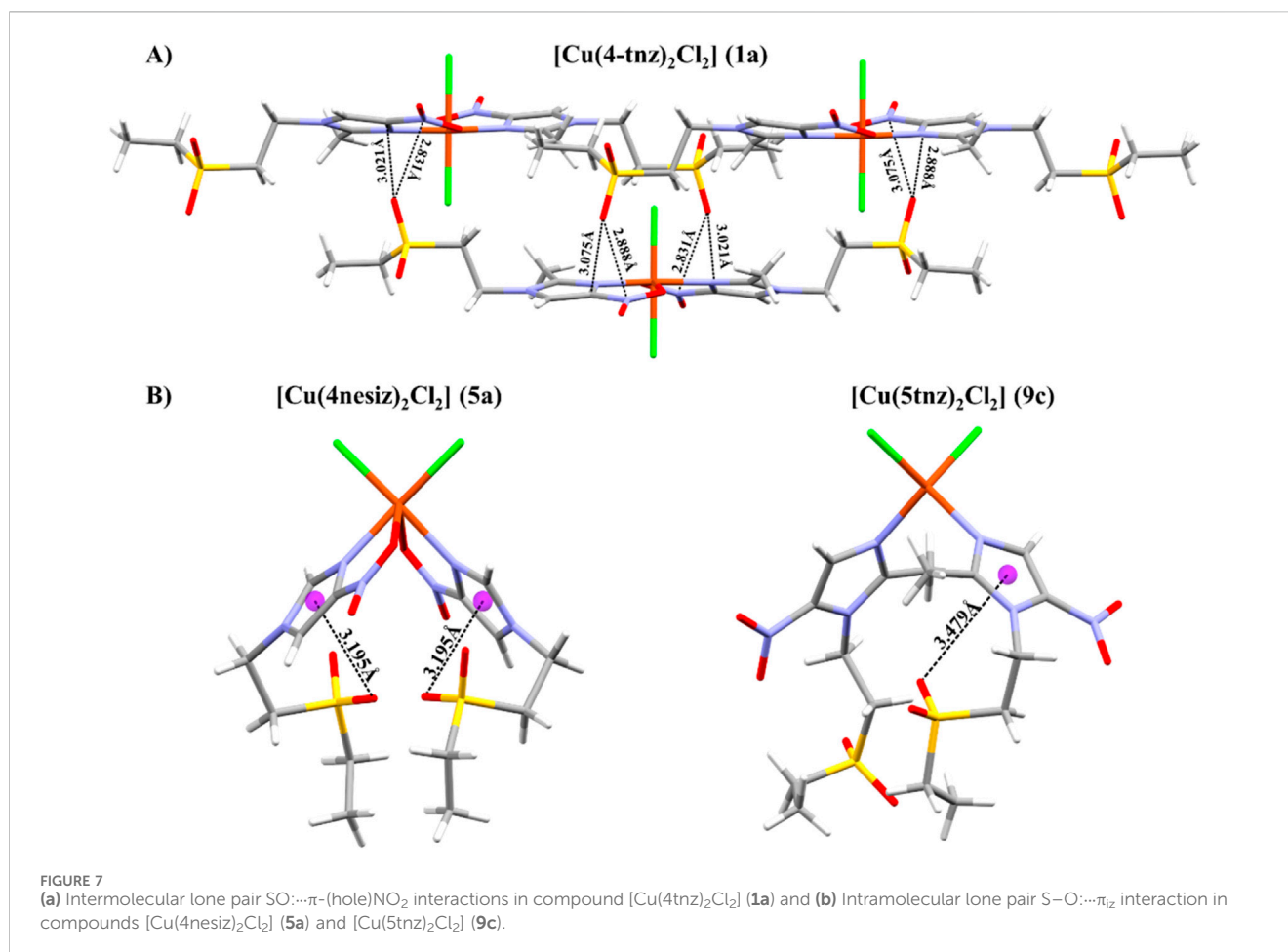


**TABLE 2** EPR data: g-values for 4-nitroimidazole copper (II) coordination compounds.

Compound	$g_z$	$g_y$	$g_x$
[Cu(4tnz) <sub>2</sub> Cl <sub>2</sub> ] ( <b>1a</b> )	2.2514	2.0588	2.0367
[Cu(4tnz) <sub>2</sub> Br <sub>2</sub> ] ( <b>1b</b> )	2.1988	2.0689	2.0689
[Cu(2m4niz) <sub>2</sub> Cl <sub>2</sub> ] ( <b>2a</b> )	2.2585	2.0639	2.0345
[Cu(2m4niz) <sub>2</sub> Br <sub>2</sub> ] ( <b>2b</b> )	2.2089	2.0632	2.0396
[Cu(4niz) <sub>2</sub> Cl <sub>2</sub> ] ( <b>4a</b> )	2.2622	2.0663	2.0360
[Cu(dmz) <sub>2</sub> Cl <sub>2</sub> ] ( <b>7a</b> )	2.2962	2.0615	2.0615
[Cu <sub>2</sub> (mnz) <sub>4</sub> ( $\mu$ -Cl) <sub>2</sub> Cl <sub>2</sub> ] ( <b>8a</b> )	2.2638	2.1492	2.1492
[Cu(mnz) <sub>2</sub> Br <sub>2</sub> ] <sub>n</sub> ( <b>8b</b> )	2.1799	2.0674	2.0674
[Cu <sub>2</sub> (tnz) <sub>4</sub> ( $\mu$ -Cl) <sub>2</sub> Cl <sub>2</sub> ] ( <b>9a</b> )	2.2328	2.0684	2.0684
[Cu(tnz) <sub>2</sub> Br <sub>2</sub> ] ( <b>9b</b> )	2.2781	2.0674	2.0674
[Cu(snz) <sub>2</sub> Cl <sub>2</sub> ] ( <b>10a</b> )	2.2049	2.0556	2.0556

The FIR spectra of the tetrahedral copper (II) complexes showed the vibration bands  $\nu$ (Cu-X), for **7a** the  $\nu$ (Cu-Cl) at 308 cm<sup>-1</sup>, and for **7b** and **9b** with  $\nu$ (Cu-Br), at 211 cm<sup>-1</sup> and 245 cm<sup>-1</sup>, respectively. The penta-coordinated binuclear

compounds [Cu<sub>2</sub>(mnz)<sub>4</sub>( $\mu$ -Cl)<sub>2</sub>Cl<sub>2</sub>] (**8a**) and [Cu<sub>2</sub>(tnz)<sub>4</sub>( $\mu$ -Cl)<sub>2</sub>Cl<sub>2</sub>] (**9a**) showed a terminal  $\nu$ (Cu-Cl) at 318 cm<sup>-1</sup> and chloro-bridged bands at 192 cm<sup>-1</sup> and 162 cm<sup>-1</sup> (Goldstein and Unsworth, 1970), while in the polymeric bromo compound **8b**,  $\nu$ (Cu-Br) was observed at 209 cm<sup>-1</sup> and  $\nu$ (Cu-O) at 319 cm<sup>-1</sup>. For the square planar compound **10a**,  $\nu$ (Cu-Cl) was assigned at 316 cm<sup>-1</sup> (Clark and Williams, 1964).

### 3.1.2.2 Electronic spectroscopy and conductivity

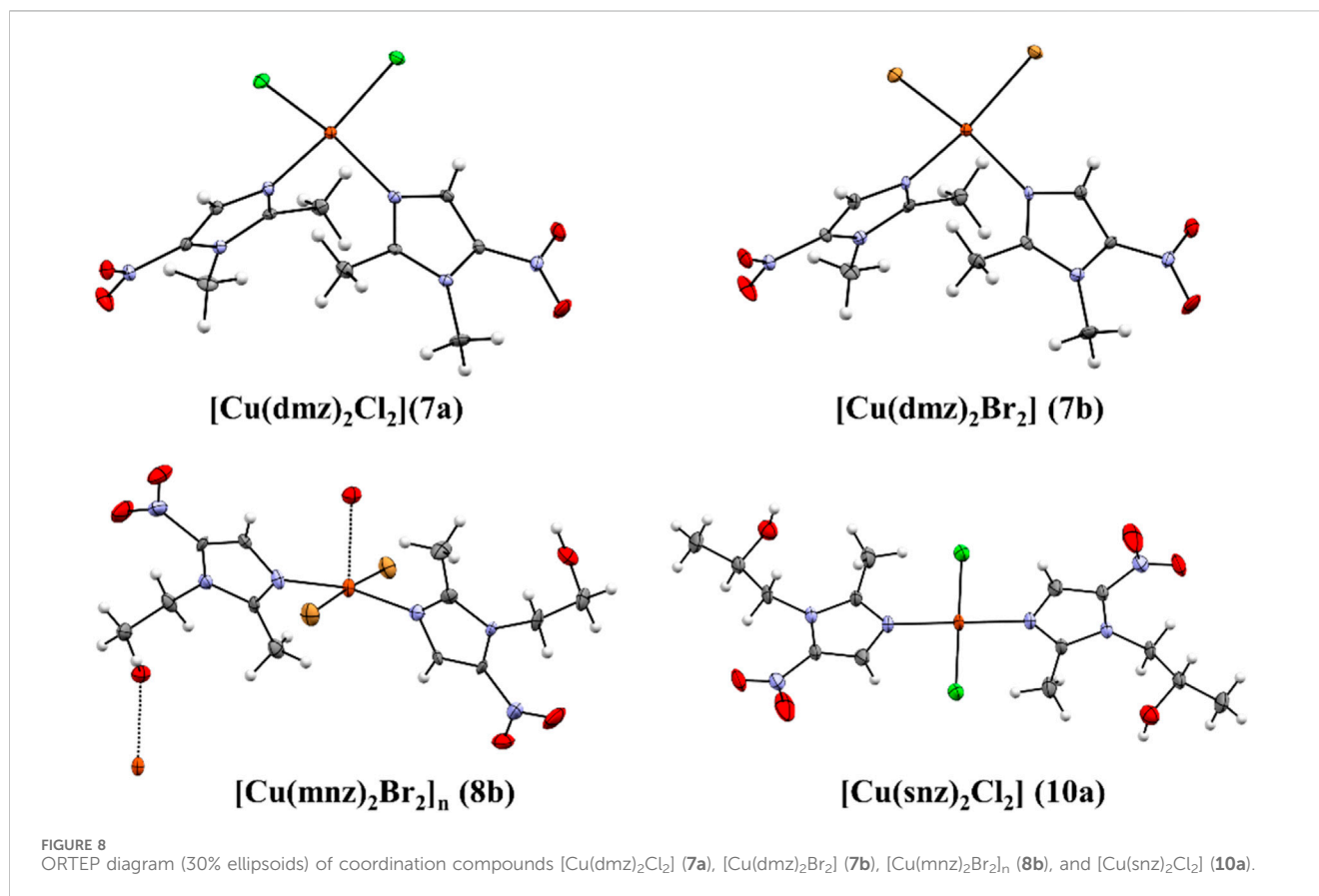
The diffuse reflectance spectra for the 5-nitroimidazole-copper (II) coordination compounds showed a single d-d electronic transition expected for a Cu(II) compound, which was highly dependent on the geometry of the metal center.

Pseudo-tetrahedral compounds [Cu(dmz)<sub>2</sub>Cl<sub>2</sub>] (**7a**), [Cu(dmz)<sub>2</sub>Br<sub>2</sub>] (**7b**), and [Cu(tnz)<sub>2</sub>Br<sub>2</sub>] (**9b**) showed a typical spectrum for this geometry, with an electronic transition at 13,000 cm<sup>-1</sup> for the chloro compound, and at ca. 10,200 cm<sup>-1</sup> for the bromo complexes. For (**7b**) and (**9b**), a second transition, in the region of 17,800 cm<sup>-1</sup>, was observed due to the distortion of the tetrahedral geometry and a weaker crystal field splitting caused by the bromo atoms. Those compounds with an SBP geometry presented an electronic transition at ca. 15,000 cm<sup>-1</sup>, [Cu(mnz)<sub>2</sub>Br<sub>2</sub>]<sub>n</sub> (**8b**) and [Cu<sub>2</sub>(tnz)<sub>4</sub>( $\mu$ -Cl)<sub>2</sub>Cl<sub>2</sub>] (**9a**), whereas in the dinuclear [Cu<sub>2</sub>(mnz)<sub>4</sub>( $\mu$ -Cl)<sub>2</sub>Cl<sub>2</sub>] (**8a**) the copper (II) atoms presented a TBP geometry with a d-d transition at 13,121 cm<sup>-1</sup>. Finally, the square planar

TABLE 3 Electronic transitions (solid state and aqueous solution) of 5-nitroimidazole compounds and molar conductivity.

Coordination compound	Solid state		Aq. solution	Conductivity Aq. solution
	$\nu_1 \text{ cm}^{-1}$	$\nu_2 \text{ cm}^{-1}$	$\nu_1 \text{ nm (cm}^{-1}\text{)}$	$\mu\text{S}\cdot\text{cm}^2\cdot\text{mol}^{-1}$
[Cu(dmz) <sub>2</sub> Cl <sub>2</sub> ] (7a)	13,009	-	762 (13,123)	258
[Cu(dmz) <sub>2</sub> Br <sub>2</sub> ] (7b)	10,239	17,828	768 (13,020)	256
[Cu <sub>2</sub> (mnz) <sub>4</sub> ( $\mu$ -Cl) <sub>2</sub> Cl <sub>2</sub> ] (8a)	13121	-	776 (12,886)	289
[Cu(mnz) <sub>2</sub> Br <sub>2</sub> ] <sub>n</sub> (8b)	15,177	-	775 (12,903)	273
[Cu <sub>2</sub> (tnz) <sub>4</sub> ( $\mu$ -Cl) <sub>2</sub> Cl <sub>2</sub> ] (9a)	15,267	-	799 (12,515)	272
[Cu(tnz) <sub>2</sub> Br <sub>2</sub> ] (9b)	10,143	17,823	788 (12,690)	260
[Cu(snz) <sub>2</sub> Cl <sub>2</sub> ] (10a)	16,255	-	N.D.	N.D.
[Cu(H <sub>2</sub> O) <sub>6</sub> ]Cl <sub>2</sub> (a)	12,500	-	808 (12,376)	256
[Cu(H <sub>2</sub> O) <sub>6</sub> ]Br <sub>2</sub> (b)	-	-	808 (12,376)	231

N.D.: not determined.



compound [Cu(snz)<sub>2</sub>Cl<sub>2</sub>] (10a) showed a broad transition centered at 16,255 cm<sup>-1</sup>. The X-ray diffraction of the complexes confirmed the proposed geometries.

Aqueous solution spectra of 5-nitroimidazole copper (II) compounds showed that the dinuclear and polymeric compounds dissociate into tetrahedral monomeric species. Additionally, the complexes presented an electrical molar

conductivity corresponding to a 1:2 electrolyte due to the exchange of the halogen atoms in aqueous solution by water molecules, as noted in Table 3.

### 3.1.2.3 X-ray studies

X-ray crystal structures of 5-nitroimidazole coordination compounds: [Cu<sub>2</sub>(mnz)<sub>4</sub>( $\mu$ -Cl)<sub>2</sub>Cl<sub>2</sub>] (8a), [Cu<sub>2</sub>(5tnz)<sub>4</sub>( $\mu$ -

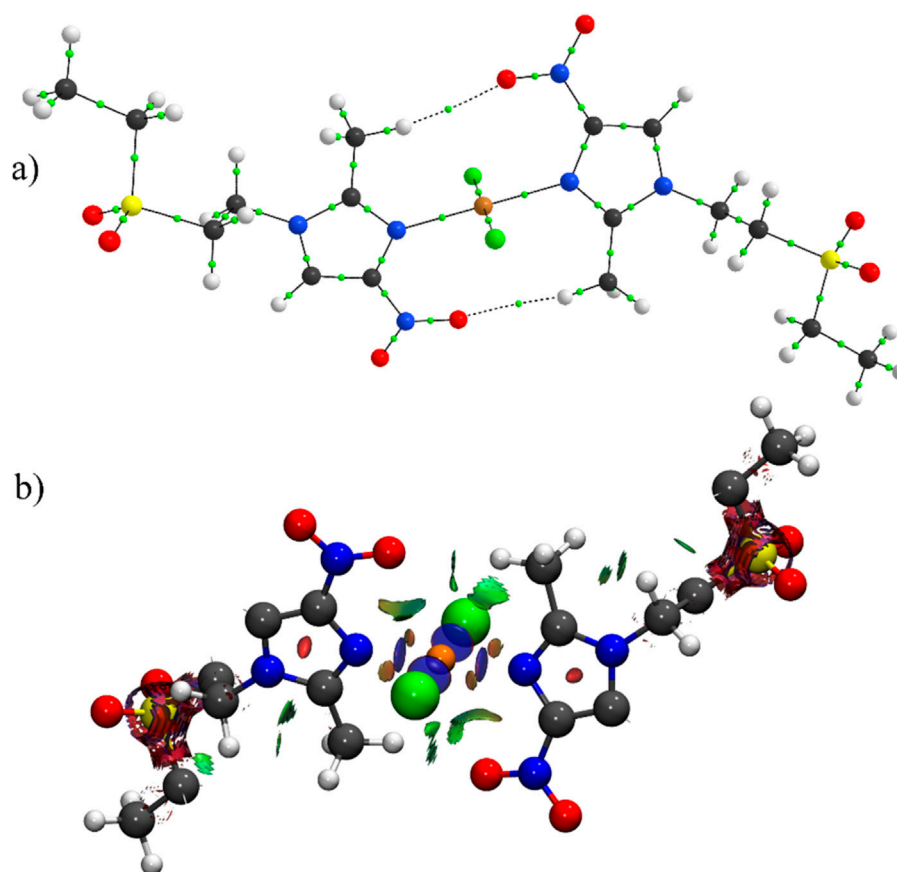


FIGURE 9  
(a) Bond critical points (green dots) and (b) NCI isosurface (0.3 a.u.) of the  $[\text{Cu}(4\text{tnz})_2\text{Cl}_2]$  (**1a**) complex.

$\text{Cl}_2\text{Cl}_2$ ) (**9a**), and  $[\text{Cu}(5\text{tnz})_2\text{Br}_2]$  (**9b**) have been reported (Navarro-Peñaloza et al., 2023a). In this work, we present four new crystal structures of the  $[\text{Cu}(\text{dmz})_2\text{Cl}_2]$  (**7a**),  $[\text{Cu}(\text{dmz})_2\text{Br}_2]$  (**7b**),  $[\text{Cu}(\text{mnz})_2\text{Br}_2]_n$  (**8b**), and  $[\text{Cu}(\text{snz})_2\text{Cl}_2]$  (**10a**) compounds.

$[\text{Cu}(\text{dmz})_2\text{Cl}_2]$  (**7a**) and  $[\text{Cu}(\text{dmz})_2\text{Br}_2]$  (**7b**) are isomorphs and crystallized in an orthorhombic system,  $\text{Aba2}$  space group. Two dmz molecules are coordinated to the copper (II) center via the N3 of the imidazole ring, with two halogens that complete the coordination sphere (Figure 8). The parameter  $\tau_4$  was calculated to determine whether the copper atom has a tetrahedral, square planar, or intermediate geometry. These compounds presented a  $\tau_4$  ( $\tau_4 = 0.45$  (**1**) and  $\tau_4 = 0.46$  (**2**)), indicative of a distorted tetrahedral geometry, as shown by the spectroscopic characterization (Yang et al., 2007).

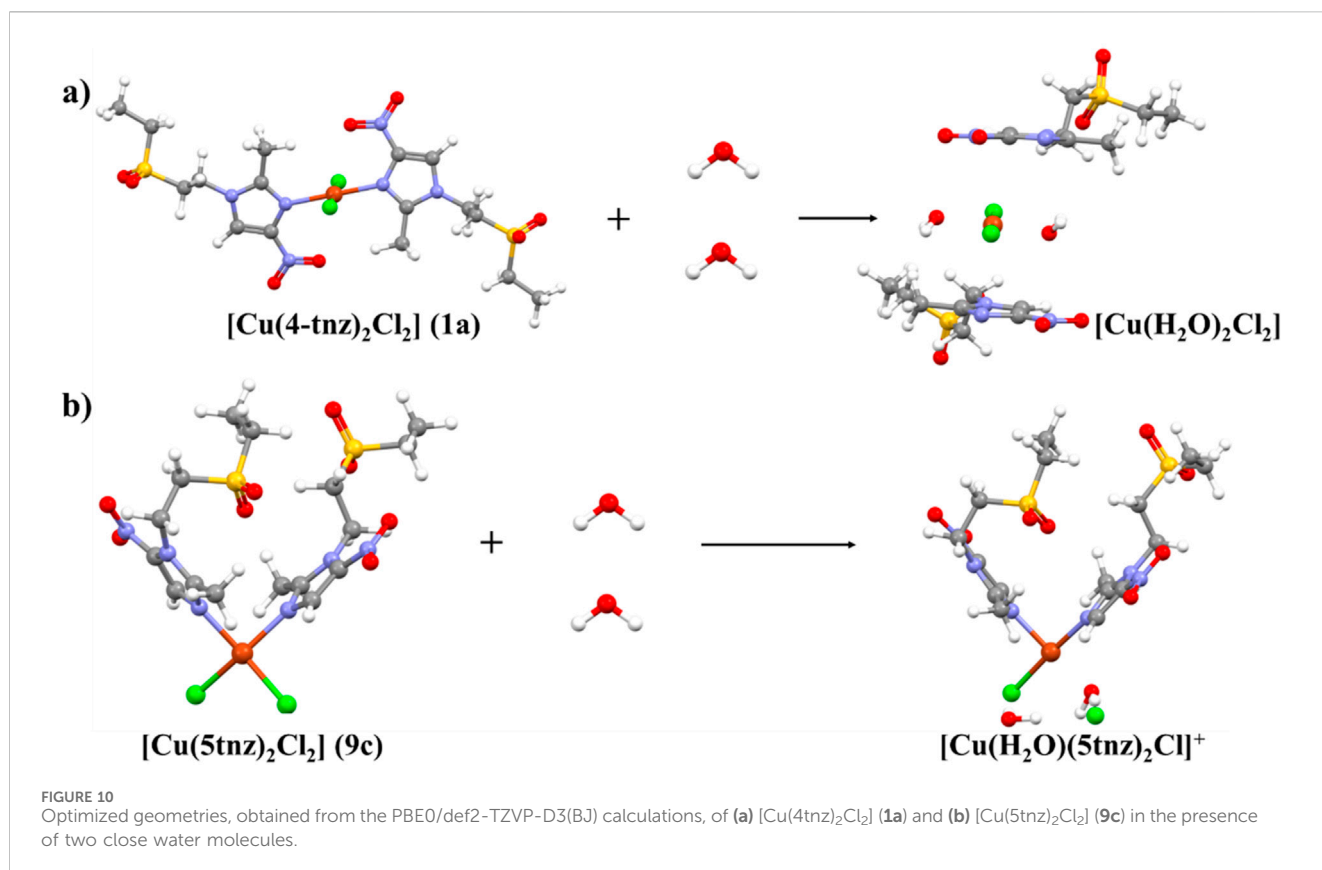
In the polymeric  $[\text{Cu}(\text{mnz})_2\text{Br}_2]_n$  (**8b**) compound, the penta-coordinated metal ion is mono-coordinated to one mnz via the N3 of the imidazole ring, while a second mnz is bridging two copper (II) atoms through the N3 of the imidazole ring and the O from the alcohol group (Cu-O: 2.443 (8) Å). Two terminal bromo atoms complete the coordination sphere. The calculated  $\tau = 0.15$  parameter indicates an SBP geometry (Addison et al., 1984).

Finally, a square planar geometry was obtained for compound  $[\text{Cu}(\text{snz})_2\text{Cl}_2]$  (**10a**). The coordination sphere of the metal ion presents two snz molecules trans to each other, through the N3 of

the imidazole ring, and two chloro atoms. The chiral carbon C8 from the snz ligands adopted an R/S configuration in the coordination compound. However, **10a** is optically inactive as there is a center of symmetry in the copper atom, being a *meso* compound.

### 3.2 Theoretical studies

It is known that the 4-nitroimidazole tautomer is favored in solution over the 5-nitroimidazole (Grimison et al., 1960). We studied both isomers with quantum calculations. The calculations showed that 4tnz (**1**) is 5 kcal/mol more stable than 5tnz (**9**). For a further understanding of this stability, the energy was partitioned to analyze the contribution from the imidazole ring, the methyl, the nitro, and the (ethylsulfonyl)ethyl groups through the QTAIM atomic energies. From this partition, it is observed that the nitro and the (ethylsulfonyl)ethyl groups are stabilized by 8.7 kcal/mol and 4.7 kcal/mol in the 5tnz (**9**) molecule, with respect to the 4tnz (**1**), while a non-significant change is observed in the methyl group for both isomers. In contrast, the imidazole ring is stabilized in 4tnz (**1**) by 17.9 kcal/mol more than in the 5tnz (**9**). Thus, the dominant effect comes from the alteration of the electronic structure of the imidazole ring upon the change in the position of the  $\text{NO}_2$  group from position 4 to 5. This trend is maintained when comparing the energies of the same groups



in the coordination compounds  $[\text{Cu}(4\text{tnz})_2\text{Cl}_2]$  (**1a**) and  $[\text{Cu}(5\text{tnz})_2\text{Cl}_2]$  (**9c**). For instance, the average energy difference between the imidazole rings is 17.8 kcal/mol,  $[\text{Cu}(4\text{tnz})_2\text{Cl}_2]$  (**1a**) being the most stable. When comparing the atomic energies of the copper atoms in both complexes, the Cu atom is stabilized by 7.3 kcal/mol in  $[\text{Cu}(5\text{tnz})_2\text{Cl}_2]$  (**9c**). This result suggests that while the stability of the ligands is not changed in the copper complexes,  $\text{Cu}^{2+}$  has a higher affinity for 5tnz than 4tnz, which could partially explain why  $[\text{Cu}(5\text{tnz})_2\text{Cl}_2]$  (**9c**) is more stable in aqueous solution.

In terms of the N $\rightarrow$ Cu and Cl $\rightarrow$ Cu coordination bonds, no significant differences were found between  $[\text{Cu}(4\text{tnz})_2\text{Cl}_2]$  (**1a**) and  $[\text{Cu}(5\text{tnz})_2\text{Cl}_2]$  (**9c**). The differences in the values of the electron density at the corresponding bond critical points (BCPs) are approximately 5%, too low to explain the variation in the reactivity of both complexes (the value of the electron density at the BCP is equivalent to the bond strength). One important result is that no BCP was found between the oxygen atom of the nitro groups and the Cu atom in  $[\text{Cu}(4\text{tnz})_2\text{Cl}_2]$  (**1a**) (Figure 9a). From the QTAIM perspective, this means that there is no formal O $\rightarrow$ Cu coordination bond. This result is corroborated by the analysis of the NCI isosurface (Figure 9b). The presence of N $\rightarrow$ Cu and Cl $\rightarrow$ Cu coordination bonds is confirmed by the appearance of the small blue disk-shaped surfaces, which are indicative of strong localized interactions. In contrast, the flat greenish surface found between the O and the Cu atoms suggests that this interaction is weaker and more delocalized, closer to a van der Waals contact. A similar conclusion was reported by Fachini et al. for compounds  $[\text{Cu}(2\text{m}4\text{niz})_2(\text{NO}_3)_2]$  and  $[\text{Cu}(2\text{m}4\text{niz})_2(\text{H}_2\text{O})_2](\text{NO}_3)_2$ , where they described the O $\rightarrow$ Cu as a weak interaction calculated with the Independent Gradient Model (IGM) and Intrinsic Bond Strength Index (IBSI) (Fachini et al.,

2023). It is noteworthy that the Cu-O weak interaction was observed by spectroscopic techniques such as FIR and UV-Vis-NIR spectroscopy, as previously discussed.

The weak nature of the O $\rightarrow$ Cu interaction in  $[\text{Cu}(4\text{tnz})_2\text{Cl}_2]$  (**1a**) may favor that solvent molecules could more easily approach the metal center. To test this hypothesis, two water molecules were placed below and above the complex, and a geometry optimization was performed. Interestingly, after doing this, not only were the water molecules coordinated to the metallic center, but the compound dissociated, as the ligands moved significantly from the metal ion (Figure 10a). When a similar calculation was performed with  $[\text{Cu}(5\text{tnz})_2\text{Cl}_2]$  (**9c**), it was observed that one of the  $\text{Cl}^-$  anions was displaced by a water molecule, thus forming a  $[\text{Cu}(\text{H}_2\text{O})(5\text{tnz})_2\text{Cl}]^+$  complex (Figure 10b), which is the precursor of the biological active Cu(I) complex  $[\text{Cu}(5\text{tnz})_2\text{Cl}]$ , described in previous works (Navarro-Peñaloza et al., 2026; Castro-Ramírez and Barba-Behrens, 2025). In sum, we propose that the low stability of  $[\text{Cu}(4\text{tnz})_2\text{Cl}_2]$  (**1a**) in aqueous solution is guided by the lower affinity of Cu(II) for the 4tnz (**1**) ligands in water, as for the weak O $\rightarrow$ Cu interaction, which favors the exchange of the two coordinated ligands by water molecules.

### 3.3 Biological studies

Four bacteria were selected to investigate the influence of the cell wall and oxygen requirements on the activity of the coordination compounds: *E. coli*, *S. aureus*, *S. mutans*, and *P. gingivalis*. The first three bacteria present an intrinsic resistance to nitroimidazole drugs. *E. coli* and *S. aureus* favor the futile cycle inactivating the prodrug

TABLE 4 Minimum bactericidal concentration for coordination compounds, ligands, and metal salts (mM).

O <sub>2</sub> requirement	Aerobic		Anaerobic	
Cell wall	G-	G+	G-	G+
Compound	<i>E. coli</i>	<i>S. aureus</i>	<i>P. gingivalis</i>	<i>S. mutans</i>
Dimetridazole (7)	NA	NA	0.012	NA
[Cu(dmz) <sub>2</sub> Cl <sub>2</sub> ] (7a)	NA	3.00	0.012	1.50
[Cu(dmz) <sub>2</sub> Br <sub>2</sub> ] (7b)	NA	3.00	0.012	0.75
Metronidazole (8)	NA	NA	0.012	NA
[Cu <sub>2</sub> (mnz) <sub>4</sub> Cl <sub>2</sub> (μ-Cl) <sub>2</sub> ] (8a)	3.00	3.00	0.012	0.75
[Cu(mnz) <sub>2</sub> Br <sub>2</sub> ] (8b)	1.50	3.00	0.012	0.37
Tinidazole (9)	NA	NA	0.012	NA
[Cu <sub>2</sub> (5tnz) <sub>4</sub> Cl <sub>2</sub> (μ-Cl) <sub>2</sub> ] (9a)	0.75	3.00	0.012	0.75
[Cu(5tnz) <sub>2</sub> Br <sub>2</sub> ] (9b)	0.75	3.00	0.012	0.75
CuCl <sub>2</sub> (a)	NA	NA	0.023	1.50
CuBr <sub>2</sub> (b)	NA	NA	0.047	0.75

NA: non-active.

activation, whereas it has been reported that *Streptococci*, such as *S. mutans*, do not possess any enzyme (nitrogenase-ferredoxin) capable of reducing the drug into the active nitroradical (Soares et al., 2012). Due to the instability of the coordination compounds with the 4-nitro derivatives, only the biological activity of the 5-nitro ligands (dmz, mnz, and 5tnz) and their copper (II) compounds was studied.

### 3.3.1 Minimum bactericidal concentration

A microdilution method was performed to screen six coordination compounds, three ligands, and the metal salts. Ligands dmz (7), mnz (8), and 5tnz (9) were active against *P. gingivalis* as the other bacteria are resistant to nitroimidazole drugs. The metal salts were active against the anaerobic bacteria, while the coordination compounds showed a better activity than the ligands and the metal salts against the four bacteria (Table 4).

Anaerobic bacteria, *S. mutans* and *P. gingivalis*, were more sensitive to the copper (II) coordination compounds, which inhibited the growth of *P. gingivalis* at a concentration of 0.012 mM, having a similar activity to that of the ligands. This is due to a great sensitivity of this bacterium to ROS as it does not possess SOD or catalase enzymes. For *S. mutans*, the copper (II) compounds were active at a higher concentration (1.50–0.37) mM, while the ligands did not present any activity. The activity shown by the complexes may be related to the disruption of the *S. mutans* zinc(II) homeostasis, as Zn-transporters in the periplasm have a higher affinity to Cu(II) ions (Garstka et al., 2025). The copper (II) compounds with mnz (8a, 8b) and 5tnz (9a, 9b) were active against both aerobic bacteria, *E. coli* and *S. aureus*. The most active compounds against the four bacteria were [Cu<sub>2</sub>(5tnz)<sub>4</sub>Cl<sub>2</sub>(μ-Cl)<sub>2</sub>] (9a) and [Cu(5tnz)<sub>2</sub>Br<sub>2</sub>] (9b). Previous work has proposed that these complexes may interact with the DNA via electrostatic interactions to damage the biomolecule (Ramírez-Palma et al., 2023; Castro-Ramírez and Barba-Behrens, 2025). However,

more experiments are needed to determine a specific mechanism of action. Based on these results, it is important to note that none of the ligands were active, except for *P. gingivalis*, while their coordination compounds showed a promising activity toward periodontal and opportunistic bacteria.

## 4 Conclusion

In this work, a series of 4- and 5-nitroimidazole derivatives and their copper (II) coordination compounds were obtained to investigate the differences in the position of the nitro group and the substituents on the chemical, structural, and biological properties.

The copper (II) complexes with the 4-nitroimidazole ligands stabilized distorted octahedral geometries for the metal ion, where the ligand is coordinated to the metal ion in a chelate mode, by an oxygen from the nitro group and the N3 of the imidazole ring, as observed in their FTIR, electronic spectroscopic, and EPR spectra, as from their X-ray crystal structures. The weak O→Cu interaction is closer to a van der Waals contact, which is reflected in the lability of their copper (II) complexes in solution. The oxygens from the SO<sub>2</sub> group may participate in non-covalent intermolecular lone pair interactions, as in compound (1a), where the nitro group from a neighboring molecule acts as an electron density acceptor, S-O:⋯π-(hole)NO<sub>2</sub>; or as an intramolecular lone pair S-O:⋯π<sub>iz</sub> interaction as in (5a).

The 5-nitro derivatives gave place to tetrahedral mononuclear compounds, with a nitrogen atom from the imidazole ligand coordinated to the metal ion. The polynuclear penta-coordinated compounds dissociated into their tetrahedral mononuclear species. In all cases, an exchange of the coordinated halogen atoms by water molecules was observed, which are biologically active species. The

5tnz copper (II) coordination compounds showed good activity toward periodontal and opportunistic bacteria, which merits further investigation.

## Data availability statement

The original contributions presented in the study are publicly available. This data can be found here: The crystallographic data for the structures have been deposited at the Cambridge Crystallographic Data Centre, [www.ccdc.cam.ac.uk/data\\_request/cif](http://www.ccdc.cam.ac.uk/data_request/cif). Accession numbers: 2498924, 2498925, 2498926, 2498927, 2498928, 2498929, 2498930, 2498931, 2498932, 2498933, 2499210. The X-ray data availability is in Section 2.3 Physical measurements: Crystallographic tables can be found in the [Supplementary Material \(Tables S1 and S2\)](#).

## Author contributions

WF: Investigation, Writing – original draft, Formal analysis, Methodology, Conceptualization. LR-C: Methodology, Writing – original draft, Investigation, Formal Analysis, Data curation. BL-R: Investigation, Software, Formal Analysis, Data curation, Methodology, Writing – original draft. AA-F: Funding acquisition, Formal Analysis, Project administration, Supervision, Writing – review and editing, Investigation, Conceptualization, Writing – original draft. NB-B: Writing – review and editing, Investigation, Writing – original draft, Supervision, Funding acquisition, Visualization, Validation, Resources, Project administration, Formal Analysis, Conceptualization.

## Funding

The author(s) declared that financial support was received for this work and/or its publication. This article through DGAPA-UNAM [IN206922] and [IT207824], as by PAIP [5000-9035] and [5000-9226].

## References

- Addison, A. W., Rao, N., Reedijk, J., and Verschoor, G. C. (1984). Synthesis, structure, and spectroscopic properties of Copper(II) compounds containing nitrogen-sulphur donor ligands; the crystal and molecular structure of Aqua[1,7-bis(N-methylbenzimidazol-2'-yl)-2,6-dithiaheptane] copper(II) perchlorate. *J. Chem. Soc. Dalton Trans.* 7, 1349–1356. doi:10.1039/DT9840001349
- Alfaro-Fuentes, I., López-Sandoval, H., Mijangos, E., Duarte-Hernández, A. M., Rodríguez-López, G., Bernal-Uruchurtu, M. I., et al. (2014). Metal coordination compounds derived from tinidazole and transition metals. Halogen and oxygen lone pair... $\pi$  interactions. *Polyhedron* 67, 373–380. doi:10.1016/j.poly.2013.09.030
- Ang, W., Jarrad, A., Cooper, M., and Blaskovich, M. (2017). Nitroimidazoles: molecular fireworks that combat a broad spectrum of infectious diseases. *J. Med. Chem.* 60, 7636–7657. doi:10.1021/acs.jmedchem.7b00143
- Anonymous (1978). The nitroimidazole family of drugs. *Brit. J. Vener. Dis.* 54, 69–71. doi:10.1136/sti.54.2.69
- Arjunan, V., Ravindran, P., Santhanam, R., Raj, A., and Mohan, S. (2012). A comparative study on vibrational, conformational and electronic structure of 1,2-dimethyl-5-nitroimidazole and 2-methyl-5-nitroimidazole. *Spectrochim. Acta A Mol. Bio. Spectrosc.* 97, 176–188. doi:10.1016/j.saa.2012.05.072
- Atria, A. M., Cortés-Cortés, P., Gardland, M. T., Baggio, R., Morales, K., Soto, M., et al. (2011). X-ray studies and antibacterial activity in copper and cobalt complexes with

## Acknowledgements

FQ-UNAM. BLR acknowledges DGTIC-UNAM (project No. LANCADUNAM-DGTIC-426) for supercomputer time. Technical support from Patricia Fierro is also acknowledged.

## Conflict of interest

The author(s) declared that this work was conducted in the absence of any commercial or financial relationships that could be construed as a potential conflict of interest.

## Generative AI statement

The author(s) declared that generative AI was not used in the creation of this manuscript.

Any alternative text (alt text) provided alongside figures in this article has been generated by Frontiers with the support of artificial intelligence and reasonable efforts have been made to ensure accuracy, including review by the authors wherever possible. If you identify any issues, please contact us.

## Publisher's note

All claims expressed in this article are solely those of the authors and do not necessarily represent those of their affiliated organizations, or those of the publisher, the editors and the reviewers. Any product that may be evaluated in this article, or claim that may be made by its manufacturer, is not guaranteed or endorsed by the publisher.

## Supplementary material

The Supplementary Material for this article can be found online at: <https://www.frontiersin.org/articles/10.3389/fchbi.2025.1736242/full#supplementary-material>

imidazole derivative ligands. *J. Chil. Chem. Soc.* 56, 786–792. doi:10.4067/S0717-97072011000300015

Bader, R. F. W., and Nguyen-Dang, T. T. (1981). Quantum theory of atoms in molecules. *Adv. Quantum Chem.* 14, 63–124. doi:10.1016/S0065-3276(08)60326-3

Bales, J. R., Mazid, M. A., Sadler, P. J., Aggarwal, A., Kuroda, R., Neidle, S., et al. (1985). Platinum(II) complexes of nitroimidazoles: synthesis, characterization, and X-ray crystal structures of cis-dichlorobis[1-(2'-hydroxyethyl)-2-hydroxymethyl-5-nitroimidazole] platinum(II) and trans-dichlorobis[1-(2'-hydroxy-3'-methoxypropyl)-2-nitroimidazole]platinum(II). *J. Chem. Soc. Dalton Trans.* 4, 795–802. doi:10.1039/DT9850000795

Barba-Behrens, N., Mutio-Rico, A. M., Joseph-Nathan, P., and Contreras, R. (1991). Preparation and characterization of new transition metal complexes of nitroimidazoles. x-ray crystal structures of two copper complexes: bis-[(p-chloro)chlorobis-(1-(2-hydroxyethyl)-2-methyl-5-nitroimidazole) copper(II)] and dichloro-bis-(2-methyl-5-nitroimidazole)copper(II). First observation of nitro group coordination to the metal ion in these heterocycles. *Polyhedron* 10, 1333–1341. doi:10.1016/S0277-5387(00)81266-8

Bharti, N., Coles, S., Hursthouse, M., Mayer, T., Gonzalez-Garza, M., Cruz-Vega, D., et al. (2002). Synthesis, crystal structure, and enhancement of the efficacy of metronidazole against *Entamoeba histolytica* by complexation with Palladium(II),

- Platinum(II), or Copper(II). *Helv. Chem. Acta* 85, 2704–2712. doi:10.1002/1522-2675(200209)85:9<2704::AID-HLCA2704>3.0.CO
- Bhujanga Rao, A. K. S., Prasad, R. S., Rao, C. G., and Singh, B. (1989). Isomerization of tinidazole involving a Novel N-Alkyl group migration. *J. Chem. Soc. Perkin Trans. 1*, 1352–1353. doi:10.1039/P19890001352
- Biswal, B. P., Panda, T., and Banerjee, R. (2012). Solution mediated phase transformation (RHO to SOD) in porous Co-imidazolate based zeolitic frameworks with high water stability. *Chem. Comm.* 48, 11868–11870. doi:10.1039/c2cc36651g
- Blaton, N. M., Peeters, O. M., and De Ranter, C. J. (1979). 2-(2-Methyl-5-nitro-1-imidazolyl)ethanol (metronidazole). *Acta Crystallogr. B Struct. Crystallogr. Cryst. Chem.* 35, 2465–2467. doi:10.1107/S0567740879009663
- Boto, R. A., Peccati, F., Laplaza, R., Quan, C., Carbone, A., Piquemal, J.-P., et al. (2020). NCIPLoT4: fast, robust, and quantitative analysis of noncovalent interactions. *J. Chem. Theory Comput.* 16, 4150–4158. doi:10.1021/acs.jctc.0c00063
- Castro-Ramírez, R., and Barba-Behrens, N. (2025). A new perspective on metal-based drugs. *Dalton Trans. Online*. doi:10.1039/d5dt01567g
- Clark, R. C., and Reid, J. S. (1995). The analytical calculation of absorption in multifaceted crystals. *Acta Crystallogr. Sect. A Found. Crystallogr.* 51, 887–897. doi:10.1107/S0108767395007367
- Clark, R. J. H., and Williams, C. S. (1964). The far-infrared spectra of metal-halide complexes of pyridine and related ligands. *Inorg. Chem.* 4, 350–357. doi:10.1021/ic50025a020
- Contini, L., Turner, R. J., and Grepioni, F. (2025). Zinc(II), copper(II) and silver(I) salicylate-metronidazole complexes as novel antimicrobial agents. *Dalton Trans.* 54, 11925–11934. doi:10.1039/d5dt01086a
- Cortés-Guzmán, F., and Bader, R. F. (2005). Complementarity of QTAIM and MO theory in the study of bonding in donor–acceptor complexes. *Coord. Chem. Rev.* 249, 633–662. doi:10.1016/j.ccr.2004.08.022
- Deo, P. N., and Dshmkh, R. (2019). Oral microbiome unveiling the fundamentals. *J. Oral Maxillofac. Pathol.* 23, 122–128. doi:10.4103/jomfp.JOMFP\_304\_18
- Desiraju, G. R., and Steiner, S. (2001). *The weak hydrogen bond in structural chemistry and biology. international union of crystallography monographs on crystallography*. New York: Oxford University Press.
- Fachini, L. G., Baptistella, G. B., Postal, K., Santana, F. S., de Souza, E. M., Ribeiro, R. R., et al. (2023). A new approach to study semi-coordination using two 2-methyl-5-nitroimidazole copper(II) complexes of biological interest as a model. *R. C. S. Adv.* 13, 27997–28007. doi:10.1039/d3ra02130k
- Flores-Leyva, S. (2018). Influence of the nitro group in the electronic and structural properties of new coordination compounds with a nitroimidazole derivative and different metal centers. (master's thesis). UNAM, Mexico.
- Freeman, C. D., Klutman, N. E., and Lamp, K. C. (1997). Metronidazole: a therapeutic review and update. *Drugs* 54, 679–708. doi:10.2165/00003495-199754050-00003
- Frisch, M. J., Trucks, G. W., Schlegel, H. B., Scuseria, G. E., Robb, M. A., Cheeseman, J. R., et al. (2016). *Gaussian 16, revision C.01*. Wallingford CT: Inc.
- Gambino, D., and Otero, L. (2019). Metal compounds in the development of antiparasitic agents: rational design from basic chemistry to the clinic. *Met. Ions Life Sci.* 19, 331–357. doi:10.1515/9783110527872-013
- Garstka, K., Hecel, A., Kozłowski, H., Dominguez-Martin, A., Szewczyk, K., and Rowińska-Żyrek, M. (2025). AdcA lipoprotein involved in Zn(II) transport in *Streptococcus mutans* – is it as metal-specific as expected? *Dalton Trans.* 54, 6795–6804. doi:10.1039/d5dt00131e
- Goldman, P. (1982). The development of 5-nitroimidazoles for the treatment and prophylaxis of anaerobic bacterial infections. *J. Antimicrob. Chemother.* 10, 23–33. doi:10.1093/jac/10.suppl\_A.23
- Goldstein, M., and Unsworth, W. D. (1970). The far-infrared spectra (450–80 cm<sup>-1</sup>) of octahedral halogen-bridged transition Metal(II) complexes. *Inorg. Chim. Acta.* 4, 342–346. doi:10.1016/S0020-1693(00)93301-2
- Goodgame, D. M. L., Page, C. J., Williams, D. J., and Stratford, I. J. (1992). Metal complexes as radiosensitizers: cobalt(II), copper(II), rhodium(II) and platinum(II) complexes of 3-(1-imidazolyl)propionic acid and some nitrosubstituted derivatives, and the crystal structure and radiosensitizer activity of [CuL<sub>2</sub>(H<sub>2</sub>O)]<sub>2</sub> where LH = 3-[1-(4-nitroimidazolyl)]propionic acid. *Polyhedron* 11, 2507–2515. doi:10.1016/S0277-5387(00)83571-8
- Granja, R. H. M. M., Nino, A. M. M., Reche, K. V. G., Giannotti, F. M., de Lima, A. C., Wanschel, A. C. B. A., et al. (2013). Determination and confirmation of metronidazole, dimetridazole, ronidazole and their metabolites in bovine muscle by LC-MS/MS. *Food Addit. Contam. Part A* 30, 970–976. doi:10.1080/19440049.2013.787653
- Greenstein, G. (1993). The role of metronidazole in the treatment of periodontal diseases. *J. Periodontol.* 64, 1–15. doi:10.1902/jop.1993.64.1.1
- Grimison, A., Ridd, J. H., and Smith, B. V. (1960). The mechanisms of N-substitution in glyoxaline derivatives. Part I. Introduction, and study of prototropic equilibria involving 4(5)-nitroglyoxaline. *J. Chem. Soc.* 0, 1352–1356. doi:10.1039/jr9600001352
- Grimme, S., Ehrlich, S., and Goerigk, L. (2011). Effect of the damping function in dispersion corrected density functional theory. *J. Comput. Chem.* 32, 1456–1465. doi:10.1002/jcc.21759
- Hübschle, C. B., Sheldrick, G. M., and Dittrich, B. (2011). ShelXle: a Qt graphical user interface for SHELXL. *J. Appl. Crystallogr.* 44, 1281–1284. doi:10.1107/S0021889811043202
- Johnson, E. R., Keinan, S., Mori-Sánchez, P., Contreras-García, J., Cohen, A. J., and Weitao, Y. (2010). Revealing noncovalent interactions. *J. Am. Chem. Soc.* 132, 6498–6506. doi:10.1021/ja100936w
- Kalinowska-Lis, U., Felczak, A., Chęcińska, L., Zawadzka, K., Patyna, E., Lisowska, K., et al. (2015). Synthesis, characterization and antimicrobial activity of water-soluble silver(I) complexes of metronidazole drug and selected counter-ions. *Dalton Trans.* 44, 8178–8189. doi:10.1039/c5dt00403a
- Krishnan, K., Chen, T., and Paster, B. J. (2017). A practical guide to the oral microbiome and its relation to health and disease. *Oral Dis.* 23, 276–286. doi:10.1111/odi.12509
- Lancini, G. C., and Lazzari, E. (1965). The synthesis of azomycin (2-Nitroimidazole). *Experientia* 21, 83. doi:10.1007/BF02144755
- Lauewaet, T., Miyamoto, Y., Ihara, S., Le, C., Kalisiak, J., Korthals, K. A., et al. (2020). Click chemistry-facilitated comprehensive identification of proteins adducted by antimicrobial 5-nitroimidazoles for discovery of alternative drug targets against giardiasis. *PLoS Negl. Trop. Dis.* 14, 1–27. doi:10.1371/journal.pntd.0008224
- Loesche, W. J., Giordano, J. R., Hujuel, P., Schwarcz, J., and Smiths, B. A. (1992). Metronidazole in periodontitis: reduced need for surgery. *J. Clin. Periodontol.* 19, 103–112. doi:10.1111/j.1600-051X.1992.tb00448.x
- Löfmark, S., Edlund, C., and Nord, C. E. (2010). Metronidazole is still the drug of choice for treatment of anaerobic infections. *Clin. Infect. Dis.* 50, S16–S23. doi:10.1086/647939
- Marenich, A. V., Cramer, C. J., and Truhlar, G. (2009). Universal solvation model based on solute electron density and on a continuum model of the solvent defined by the bulk dielectric constant and atomic surface tensions. *J. Phys. Chem. B* 113, 6378–6396. doi:10.1021/jp810292n
- Melo, M. A. S., Martini-Garcia, I., Alluhaidan, T., Qaw, M., Montoya, C., Orrego, S., et al. (2025). The next frontier in antibacterial dental resins: a 20-year journey of innovation and expectations. *Dent. Mat.* 41, 1045–1057. doi:10.1016/j.dental.2025.06.013
- Mittal, S., and Mallia, M. B. (2023). Molecular imaging of tumor hypoxia: evolution of nitroimidazole radiopharmaceuticals and insights for future development. *Bioorg. Chem.* 139, 106687. doi:10.1016/j.bioorg.2023.106687
- Mittal, S., Kumar, C., Jha, L., and Mallia, M. B. (2024). A thiourea-bridged <sup>99m</sup>Tc(CO)<sub>3</sub>-dipicolylamine-2-nitroimidazole complex for targeting tumor hypoxia: utilizing metabolizable thiourea-bridge to improve pharmacokinetics. *Drug Dev. Res.* 85, e22258. doi:10.1002/ddr.22258
- Montoya, C., Roldan, L., Yu, M., Valliani, S., Ta, C., Yang, M., et al. (2023). Smart dental materials for antimicrobial applications. *Bioact. Mater.* 24, 1–19. doi:10.1016/j.bioactmat.2022.12.002
- Mudde, S. E., Upton, A. M., Lenaerts, A., Bax, H. I., and De Steenwinkel, J. E. M. (2022). Delamanid or pretomanid? A solomonic judgement. *J. Antimicrob. Chemother.* 77, 880–902. doi:10.1093/jac/dkab505
- Müller-Kratz, J., Garcia-Bournissen, F., Frolyth, C. J., and Sosa-Estani, S. (2018). Clinical and pharmacological profile of benzimidazole for treatment of chagas disease. *Expert Rev. Clin. Pharmacol.* 11, 943–957. doi:10.1080/17512433.2018.1509704
- Nakamura, S. (1955). Structure of azomycin, a new antibiotic. *Pharm. Bull.* 3, 379–383. doi:10.1248/cpb1953.3.379
- Navarro-Peñaloza, R., Landeros-Rivera, B., López-Sandoval, H., Castro-Ramírez, R., and Barba-Behrens, N. (2023a). New insights on transition metal coordination compounds with biological active azole and nitroimidazole derivatives. *Coord. Chem. Rev.* 494, 215360. doi:10.1016/j.ccr.2023.215360
- Navarro-Peñaloza, R., Anacleto-Santos, J., Rivera-Fernández, N., Sanchez-Bartez, F., Gracia-Mora, I., Caballero, A. B., et al. (2023b). Anti-toxoplasma activity and DNA-Binding of copper(II) and zinc(II) coordination compounds with 5-nitroimidazole-based ligands. *J. Biol. Inorg. Chem.* 29, 33–49. doi:10.1007/s00775-023-02029-7
- Navarro-Peñaloza, R., Landeros-Rivera, B., Palacios-Ramírez, J. I., Sánchez-Bartéz, F., Gracia-Mora, I., González, F. J., et al. (2026). Contribution of copper(II) and zinc(II) to the electrochemical and biological properties of 5-nitroimidazole coordination compounds. An experimental and theoretical approach. *J. Inorg. Biochem.* 274, 113075. doi:10.1016/j.jinorgbio.2025.113075
- Nepali, K., Lee, H., and Liou, J. (2019). Nitro-group-containing drugs. *J. Med. Chem.* 62, 2851–2893. doi:10.1021/acs.jmedchem.8b00147
- Nguyen, A. T., and Kim, H. (2023). Recent developments in PET and SPECT radiotracers as radiopharmaceuticals for hypoxia tumors. *Pharmaceutics* 15, 1840. doi:10.3390/pharmaceutics15071840
- Ozasa, T., Mizutani, M., Nishihara, T., Suzuki, M., and Tanabe, K. (2025). Preparation of <sup>18</sup>B-enriched nitroimidazole derivative by click reaction as a functional drug for

- hypoxia-targeting boron-neutron capture therapy. *Results Chem.* 15, 102245. doi:10.1016/j.rechem.2025.102245
- Paz-Díaz, B., Vázquez-Olmos, A., Almaguer-Flores, A., García-Pérez, V., Sato-Berrú, R. Y., Almanza-Arjona, Y. C., et al. (2023). ZnFe<sub>2</sub>O<sub>4</sub> and CuFe<sub>2</sub>O<sub>4</sub> nanocrystals: synthesis, characterization, and bactericidal application. *J. Clust. Sci.* 34, 111–119. doi:10.1007/s10876-021-02203-4
- Peres, M. A., Macpherson, L. M., Weyant, R. J., Daly, B., Venturelli, R., Mathur, M. R., et al. (2019). Oral diseases: a global public health challenge. *Lancet* 394, 249–260. doi:10.1016/S0140-6736(19)31146-8
- Poyraz, S., Yildirim, M., and Ersatir, M. (2024). Recent pharmacological insights about imidazole hybrids: a comprehensive review. *Med. Chem. Res.* 33, 839–868. doi:10.1007/s00044-024-03230-2
- Radko, L., Stypuła-Trębas, S., Posyniak, A., Żyro, D., and Ochocki, J. (2019). Silver(I) complexes of the pharmaceutical agents metronidazole and 4-Hydroxymethylpyridine: comparison of cytotoxic profile for potential clinical application. *Molecules* 24, 1949–1961. doi:10.3390/molecules24101949
- Rajendran, J. G., and Krohn, K. A. (2005). Imaging hypoxia and angiogenesis in tumors. *Radiol. Clin. N. Am.* 43, 169–187. doi:10.1016/j.rcl.2004.08.004
- Ramírez-Palma, L. G., Castro-Ramírez, R., Lozano-Ramos, L., Galindo-Murillo, R., Barba-Behrens, N., and Cortés-Guzmán, F. (2023). DNA recognition site of anticancer tinidazole copper(II) complexes. *Dalton Trans.* 52, 2087–2097. doi:10.1039/D2DT02854A
- Reyes-Carmona, L., Sepúlveda-Robles, O. A., Almaguer-Flores, A., Bello-Lopez, J. M., Ramos-Vilchis, C., and Rodil, S. E. (2023). Antimicrobial activity of silver-copper coating against aerosols containing surrogate respiratory viruses and bacteria. *PLoS ONE* 18, e0294972. doi:10.1371/journal.pone.0294972
- Rochon, F. D., Kong, P., Melanson, R., Skov, K. A., and Farrell, N. (1991). Characterization and properties of monoamine nitroimidazole complexes of platinum[PtCl<sub>2</sub>(NH<sub>3</sub>)(NO<sub>2</sub>Im)]. Crystal and molecular structure of *cis*-Amminedichloro-1-((2-hydroxyethyl)amino)carbonylmethyl-2-nitroimidazole platinum(II). *Inorg. Chem.* 30, 4531–4535. doi:10.1021/ic00024a013
- Rochon, F. D., Melanson, R., and Farrell, N. (1993). Structures of the nitroimidazole platinum group metal complexes *cis*-Amminedibromo[1-((2-hydroxyethyl)amino)carbonylmethyl-2-nitroimidazole]-platinum(II) and *trans*-Dichlorobis(1-hydroxyethyl-2-methyl-5-nitroimidazole)-palladium(II). *Acta Cryst. Sec. C* 49, 1703–1706. doi:10.1107/S0108270193002537
- Rolfe, R., and Finegold, S. (1981). Comparative *in vitro* activity of new beta-lactam antibiotics against anaerobic bacteria. *Antimicrob. Agents Chemother.* 20, 600–609. doi:10.1128/aac.20.5.600
- Ruan, Q., Liu, Y., Liao, L., Jiang, Y., Jiang, J., Zhang, J., et al. (2023). Synthesis and evaluation of <sup>99m</sup>Tc-Labelled 2-Nitroimidazole derivatives with different linkers for tumour hypoxia imaging. *Pharm* 16, 1276–1290. doi:10.3390/ph16091276
- Salazar-Cano, J. R., Guevara-García, A., Vargas, R., Restrepo, A., and Garza, J. (2016). Hydrogen bonds in methane–water clusters. *Phys. Chem. Chem. Phys.* 18, 23508–23515. doi:10.1039/c6cp04086a
- Samuelson, J. (1999). Why metronidazole is active against both bacteria and parasites. *Antimicrob. Agents Chemother.* 43, 1533–1541. doi:10.1128/aac.43.7.1533
- Ségalas, I., and Beuchamp, A. (1991). Preparation and structure of silver complexes with 4-nitroimidazole. *Can. J. Chem.* 70, 943–951. doi:10.1139/v92-127
- Sheldrick, G. M. (2008). A short history of SHELX. *Acta Crystallogr. Sect. A Found. Crystallogr.* 64, 112–122. doi:10.1107/S0108767307043930
- Soares, G. M. S., Figueiredo, L. C., Faveri, M., Cortelli, S. C., Duarte, P. M., and Feres, M. (2012). Mechanisms of action of systemic antibiotics used in periodontal treatment and mechanisms of bacterial resistance to these drugs. *J. Appl. Oral Sci.* 20, 295–309. doi:10.1590/S1678-77572012000300002
- Suárez, L. J., Arce, R. M., Gonçalves, C., Pinheiro-Furquim, C., Casto-Dos Santos, N., Reramal-Valdes, B., et al. (2024). Metronidazole may display anti-inflammatory features in periodontitis treatment: a scoping review. *Mol. Oral Microbiol.* 39, 240–259. doi:10.1111/omi.12459
- Todd, A. J., and Gristmill, T. K. (2019). Software, Overland Park KS, USA, (aim.tkgristmill.com).
- Turner, R. J. (2024). The good, the bad and the ugly of metals as antimicrobials. *Biometals* 37, 545–559. doi:10.1007/s10534-023-00565-y
- Varga, N., Smiesko, M., Jiang, X., Jakob, R. P., Wagner, B., Mühlethaler, T., et al. (2024). Strengthening an intramolecular non-classical hydrogen bond to get in shape for binding. *Angew. Chem. Int. Ed.* 63, e202406024. doi:10.1002/anie.202406024
- Vichi-Ramírez, M. M., López-López, E., Soriano-Correa, C., and Barrientos-Salcedo, C. (2024). Using 5-Nitroimidazole derivatives against neglected tropical protozoan diseases: systematic review. *Future Pharmacol.* 4, 222–255. doi:10.3390/futurepharmacol4010015
- Wang, J., Li, C., Bai, C., Hu, H., and Xue, G. (2017). Selective fluorescence sensors and photocatalysis of four new luminescent coordination complexes. *J. Mol. Struct.* 1141, 107–114. doi:10.1016/j.molstruc.2017.03.094
- Wardman, P., and Clarke, E. D. (1975). One-electron reduction potentials of substituted nitroimidazoles measured by pulse radiolysis. *J. Chem. Soc. Faraday Trans. 1* (72), 1377–1390. doi:10.1039/F19767201377
- Wilkinson, S. R., Taylor, M. C., Horn, D., Kelly, J. M., and Cheeseman, I. (2008). A mechanism for cross-resistance to nifurtimox and benznidazole in trypanosomes. *Proc. Natl. Acad. Sci.* 105, 5022–5027. doi:10.1073/pnas.0711014105
- Willis, J. R., and Gabaldón, T. (2020). The human oral microbiome in health and disease: from sequences to ecosystems. *Microorganisms* 8, 308. doi:10.3390/microorganisms8020308
- Wood, S. G., John, B. A., Chasseaud, L. F., Brodie, R. R., Baker, J. M., Faulkner, J. K., et al. (1986). Pharmacokinetics and metabolism of <sup>14</sup>C-tinidazole in humans. *J. Antimicrob. Chemother.* 17, 801–809. doi:10.1093/jac/17.6.801
- Yang, L., Powell, D. R., and Houser, R. P. (2007). Structural variation in copper(I) complexes with pyridylmethylamide ligands: structural analysis with a new four-coordinate geometry index. *T<sub>4</sub> Dalton Trans.* 9, 955–964. doi:10.1039/B617136B